
Constant Time Graph Neural Networks

Ryoma Sato^{1,2} Makoto Yamada^{1,2,3} Hisashi Kashima^{1,2}

Abstract

The recent advancements in graph neural networks (GNNs) have led to state-of-the-art performances in various applications, including cheminformatics, question-answering systems, and recommender systems. However, scaling up these methods to huge graphs, such as social networks and Web graphs, remains a challenge. In particular, the existing methods for accelerating GNNs either are not theoretically guaranteed in terms of the approximation error or incur at least a linear time computation cost. In this study, we reveal the query complexity of the uniform node sampling scheme for Message Passing Neural Networks including GraphSAGE, graph attention networks (GATs), and graph convolutional networks (GCNs). Surprisingly, our analysis reveals that the complexity of the node sampling method is completely independent of the number of the nodes, edges, and neighbors of the input and depends only on the error tolerance and confidence probability while providing a theoretical guarantee for the approximation error. To the best of our knowledge, this is the first paper to provide a theoretical guarantee of approximation for GNNs within constant time. Through experiments with synthetic and real-world datasets, we investigated the speed and precision of the node sampling scheme and validated our theoretical results.

1. Introduction

Machine learning on graph structures has various applications, such as chemo-informatics (Gilmer et al., 2017; Zhang et al., 2018), question answering systems (Schlichtkrull et al., 2018; Park et al., 2019), and recommender systems (Ying et al., 2018; Wang et al., 2019a;b; Fan et al., 2019). Recently, a novel machine learning model for graph data called graph neural networks (GNNs)

(Gori et al., 2005; Scarselli et al., 2009) demonstrated state-of-the-art performances in various graph learning tasks. However, large scale graphs, such as social networks and Web graphs, contain billions of nodes, and even a linear time computation cost per iteration is prohibitive. Therefore, the application of GNNs to huge graphs presents a challenge. Although Ying et al. (2018) succeeded in applying GNNs to a Web-scale network using MapReduce, their method still requires massive computational resources.

There are several node sampling techniques for reducing GNN computation. For example, an empirical neighbor sampling scheme is used to speed up GraphSAGE (Hamilton et al., 2017). FastGCN employs a random layer-wise node sampling (Chen et al., 2018a). Huang et al. (2018) further improved FastGCN by using an adaptive sampling technique to reduce the variance of estimators. Chen et al. (2018b) proposed a variant of neighbor sampling, which used historical activations to reduce the estimator variance. ClusterGCN (Chiang et al., 2019) clusters nodes into dense blocks and aggregates features within each block. LADIES (Zou et al., 2019) combines layer-wise sampling with neighbor sampling to improve efficiency. Overall, the existing sampling techniques for GNNs are effective in practice. However, these techniques either are not theoretically guaranteed in terms of approximation error or incur at least a linear time computation cost.

In this study, we considered the problem of approximating the embedding of *one* node using GNNs *in constant time* with maximum precision¹. We analyzed the neighbor sampling technique (Hamilton et al., 2017) to show that only a constant number of samples is needed to guarantee the approximation error for Message Passing Neural Networks (Gilmer et al., 2017) including GraphSAGE (Hamilton et al., 2017), GATs (Veličković et al., 2018), and GCNs (Kipf & Welling, 2017). It should be noted that the neighbor sampling technique was introduced as a heuristic method originally, and no theoretical guarantees were

¹Kyoto University ²RIKEN AIP ³JST PRESTO. Correspondence to: Ryoma Sato <r.sato@ml.ist.i.kyoto-u.ac.jp>.

¹E.g., the problem of predicting whether a user of an SNS clicks an advertisement using GNNs in real time (i.e., when the user accesses the SNS). A user may have many neighbors, but GNNs must respond within a limited time, which prohibits exact computation. This motivated us to approximate the exact computation in limited time with a theoretical guarantee.

provided. Specifically, we prove PAC learning-like bounds of the approximation errors of neighbor sampling. Given an error tolerance ε and confidence probability $1 - \delta$, our analysis shows that the estimate \hat{z}_v of the exact embedding z_v of a node v , such that $\Pr[\|\hat{z}_v - z_v\|_2 \geq \varepsilon] \leq \delta$, and the estimate $\widehat{\frac{\partial z_v}{\partial \theta}}$ of the exact gradient $\frac{\partial z_v}{\partial \theta}$ of the embedding z_v with respect to the network parameters θ , such that $\Pr[\|\widehat{\frac{\partial z_v}{\partial \theta}} - \frac{\partial z_v}{\partial \theta}\|_F \geq \varepsilon] \leq \delta$, can be computed in constant time. In particular, the uniform node sampling can approximate the exact embedding and its gradients within $O(\frac{1}{\varepsilon^2 L} (\log \frac{1}{\varepsilon} + \log \frac{1}{\delta})^{L-1} \log \frac{1}{\delta})$ time, where L denotes the number of layers. This complexity is completely independent of the number of the nodes, edges, and neighbors of the input, which enables us to deal with graphs irrespective of their size. Moreover, the complexity is a polynomial with respect to $\frac{1}{\varepsilon}$ and $\log \frac{1}{\delta}$. We demonstrate that the time complexity is optimal when $L = 1$ with respect to the error tolerance ε . Our analysis can be applied to the prediction setting by considering the prediction problem as 1-dimensional embedding in $[0, 1]$. In that case, the prediction with the approximation is correct if the exact computation predicts correctly with margin ε .

In addition to presenting positive results, we show that some existing GNNs, including the original GraphSAGE (Hamilton et al., 2017), cannot be approximated in constant time by any algorithm. Our theoretical results not only provide guarantees of approximation errors but also reveal which information each GNN model gives importance to in the light of the computational complexity. The GNN architectures that can be approximated in constant time do not use the fine-grained information but only the coarse information of the input graph, whereas the GNN architectures that cannot be approximated in constant time do use all the information of the input graph. These observations provide theoretical characteristics of GNN architectures.

We experimentally show the validity of our theories including negative results, and we show that the approximation error between the exact computation and its approximation rapidly converges to zero when possible. To the best of our knowledge, this is the first analysis concerning constant time approximation for GNNs with a theoretical guarantee.

Contributions:

- We analyze the neighbor sampling technique for GraphSAGE, graph attention networks (GATs), and GCNs to provide theoretical justification. In particular, our analysis shows that the complexity is completely independent of the number of nodes, edges, and neighbors of the input.
- We show that some existing GNNs, including the original GraphSAGE (Hamilton et al., 2017), cannot be

approximated in constant time by any algorithm (see Table 1 for details).

- We empirically validate our theorems using synthetic and real-world datasets.

2. Related Work

2.1. Graph Neural Networks (GNNs)

Originally, GNN-like models were proposed in the chemistry field (Sperduti & Starita, 1997; Baskin et al., 1997). Sperduti & Starita (1997) applied a linear aggregation operation and a non-linear activation function recursively, and Baskin et al. (1997) utilized parameter sharing to model invariant transformations on node and edge features. These features are common in modern GNNs. Gori et al. (2005) and Scarselli et al. (2009) proposed novel graph learning models and named them graph neural networks (GNNs). Their models recursively apply the propagation function until convergence to obtain node embeddings. Li et al. (2016) improved their models to create gated graph neural networks by introducing LSTM and GRU. Molecular graph networks (Merkwirth & Lengauer, 2005) is a concurrent model of the GNNs (Gori et al., 2005) with similar architecture, but they use a constant number of layers. Duvenaud et al. (2015) constructed a GNN model based on circular fingerprints. Bruna et al. (2014) and Defferrard et al. (2016) took advantage of graph spectral analysis and graph signal processing to construct GNN models. Kipf & Welling (2017) proposed GCNs, which significantly outperform the existing methods, including non-neural network-based approaches. They approximate a spectral model by linear functions with respect to the graph Laplacian and reduced spectral models to spatial models. Gilmer et al. (2017) proposed message passing neural networks (MPNNs), a general framework of GNNs using the message passing mechanism. GATs (Veličković et al., 2018) improve the performance of GNNs greatly by incorporating the attention mechanism. With the advent of GATs, various GNN models with the attention mechanism have been proposed (Wang et al., 2019a; Park et al., 2019). Recently, the expressive power of GNNs has been revealed theoretically. For example, Xu et al. (2019) and Morris et al. (2019) showed that the expressive power of message passing GNNs is at most the power of the WL-1 test (Weisfeiler & Lehman, 1968). Sato et al. (2019) showed that the set of problems that message passing GNNs can solve is the same as that which can be solved by distributed local algorithms (Angluin, 1980; Suomela, 2013).

GraphSAGE (Hamilton et al., 2017) is an additional GNN model, which employs neighbor sampling to reduce the computational costs of training and inference. Neighbor

Table 1. ✓ indicates that *neighbor sampling* approximates the network in constant time. ✗ indicates that *no algorithm* can approximate the network in constant time. ✓ in the Gradient column indicates that the error between the gradient of the approximated embedding and that of the exact embedding is also theoretically bounded. ✓* requires an additional condition to approximate it in constant time.

Activation	GATs, GraphSAGE-GCN, GraphSAGE-mean		GraphSAGE-pool	GCNs	
	Embedding	Gradient		Embedding	Gradient
sigmoid / tanh	✓ Thm. 1	✓ Thm. 4	✗ Thm. 9	✓* Thm. 1	✓* Thm. 4
ReLU	✓ Thm. 1	✗ Thm. 8	✗ Thm. 9	✓* Thm. 1	✗ Thm. 8
ReLU + normalization	✗ Thm. 7	✗ Thm. 7	✗ Thm. 9	✗ Thm. 7	✗ Thm. 7

sampling enables GraphSAGE to deal with large graphs. However, neighbor sampling was introduced without any theoretical guarantee, and the number of samples is chosen empirically. An alternative computationally efficient GNN would be FastGCN (Chen et al., 2018a), which employs layer-wise random node sampling to speed up training and inference. Huang et al. (2018) further improved FastGCN by using an adaptive node sampling technique to reduce the variance of estimators. By virtue of the adaptive sampling technique, it reduces the computational costs and outperforms neighbor sampling in terms of classification accuracy and convergence speed. Chen et al. (2018b) proposed an alternative neighbor sampling technique, which uses historical activations to reduce the estimator variance. Additionally, it can achieve zero variance after a certain number of iterations. However, because it uses the same sampling technique as GraphSAGE to obtain the initial solution, the approximation error is not theoretically bounded until the $\Omega(n)$ -th iteration. ClusterGCN (Chiang et al., 2019) first clusters nodes into dense blocks and then aggregates node features within each block. LADIES (Zou et al., 2019) samples neighboring nodes using importance sampling for each layer to improve efficiency while keeping variance small. However, neither LADIES (Zou et al., 2019) nor ClusterGCN (Chiang et al., 2019) has a theoretical guarantee on the approximation error. Overall, the existing sampling techniques are effective in practice. However, they either are not theoretically guaranteed in terms of approximation error or incur at least a linear time computation cost to calculate the embedding of a node and its gradients.

2.2. Sublinear Time Algorithms

Sublinear time algorithms were originally proposed for property testing (Rubinfeld & Sudan, 1996). Sublinear property testing algorithms determine whether the input has some property π or the input is sufficiently far from property π with high probability in sublinear time with respect to the input size. Sublinear time approximation algorithms are an additional type of sublinear time algorithms. More specifically, they calculate a value sufficiently close to the exact value with high probability in sublinear time.

Constant time algorithms are a subclass of sublinear time algorithms. They operate not only in sublinear time with respect to the input size but also in constant time. The proposed algorithm is classified as a constant time approximation algorithm.

The examples of sublinear time approximation algorithms include minimum spanning tree in metric space (Czumaj & Sohler, 2004) and minimum spanning tree with integer weights (Chazelle et al., 2005). Parnas & Ron (2007) proposed a method to convert distributed local algorithms into constant time approximation algorithms. In their paper, they proposed a method to construct constant time algorithms for the minimum vertex cover problem and dominating set problem. Nguyen & Onak (2008) and Yoshida et al. (2009) improved the complexities of these algorithms. A classic example of sublinear time algorithms related to machine learning includes clustering (Indyk, 1999; Mishra et al., 2001). Examples of recent studies in this stream include constant time approximation of the minimum value of quadratic functions (Hayashi & Yoshida, 2016) and constant time approximation of the residual error of the Tucker decomposition (Hayashi & Yoshida, 2017). Hayashi and Yoshida adopted simple sampling strategies to obtain a theoretical guarantee, as we did in our study. In this paper, we provide a theoretical guarantee for the approximation of GNNs within constant time for the first time.

3. Background

3.1. Notations

Let G the input graph, $\mathcal{V} = \{1, 2, \dots, n\}$ the set of nodes, $n = |\mathcal{V}|$ the number of nodes, \mathcal{E} the set of edges, $m = |\mathcal{E}|$ the number of edges, $\deg(v)$ the degree of node v , $\mathcal{N}(v)$ the set of neighbors of a node v , $\mathbf{x}_v \in \mathbb{R}^{d_0}$ the feature vector associated to a node $v \in \mathcal{V}$, and $\mathbf{X} = (\mathbf{x}_1, \mathbf{x}_2, \dots, \mathbf{x}_n)^\top \in \mathbb{R}^{n \times d_0}$ the stacked feature vectors, and let $^\top$ denote the matrix transpose.

3.2. Node Embedding Model

Algorithm 1 \mathcal{O}_z : Exact embedding

Require: Graph $G = (\mathcal{V}, \mathcal{E})$; Features $\mathbf{X} \in \mathbb{R}^{n \times d_0}$; Node index $v \in \mathcal{V}$; Model parameters θ .

Ensure: Exact embedding z_v

```

1:  $z_i^{(0)} \leftarrow x_i \ (\forall i \in \mathcal{V})$ 
2: for  $l \in \{1, \dots, L\}$  do
3:   for  $i \in \mathcal{V}$  do
4:      $h_i^{(l)} \leftarrow \sum_{u \in \mathcal{N}(i)} M_{liu}(z_i^{(l-1)}, z_u^{(l-1)}, e_{iu}, \theta)$ 
5:      $z_i^{(l)} \leftarrow U_l(z_i^{(l-1)}, h_i^{(l)}, \theta)$ 
6:   end for
7: end for
8: return  $z_v^{(L)}$ 
    
```

We consider the node embedding problem using GNNs with MPNN framework (Gilmer et al., 2017). This framework includes many GNN models, such as GraphSAGE and GCNs. Algorithm 1 shows the algorithm of MPNNs. We refer to $z_v^{(L)}$ as z_v for the sake of simplicity. The aim of this study was to show that it is possible to approximate the embedding vector z_v and gradients $\frac{\partial z_v}{\partial \theta}$ in constant time with the given model parameters θ and node v .

3.3. Computational Model Assumptions

In the design of constant time algorithms, we need to specify a means by which they can access the input, because they cannot read the entire input. We follow the standard convention of sublinear time algorithms (Parnas & Ron, 2007; Nguyen & Onak, 2008). We model an algorithm as an oracle machine that can generate queries regarding the input and we measure the complexity by query complexity. Algorithms can access the input only by querying the following oracles: (1) $\mathcal{O}_{\text{deg}}(v)$: the degree of node v , (2) $\mathcal{O}_G(v, i)$: the i -th neighbor of node v , and (3) $\mathcal{O}_{\text{feature}}(v)$: the feature of node v . We assume that an algorithm can query the oracles in constant time per query.

3.4. Problem Formulation

In this paper, we aim to compute an embedding of a single node in constant time because it is useful in online settings as we introduced in the footnote of the introduction. In some applications, computing embeddings of all nodes is required. In such cases, embeddings can be computed in $O(n)$ time if each embedding can be computed in constant time, while exact computation requires at least $O(m)$ time, which is large if the input graph is dense.

Formally, given a node v , we compute the following functions with the least number of oracle accesses: (1) $\mathcal{O}_z(v)$: the embedding z_v and (2) $\mathcal{O}_g(v)$: the gradients of parameters $\frac{\partial z_v}{\partial \theta}$. However, the exact computation of \mathcal{O}_z and \mathcal{O}_g requires at least $\text{deg}(v)$ queries to aggregate the features from the neighbor nodes, which is not constant time with

respect to the input size. Thus, it is computationally expensive to execute the algorithm for a very large network, which motivates us to make the following approximations.

- $\hat{\mathcal{O}}_z(v, \varepsilon, \delta)$: an estimate \hat{z}_v of z_v such that $\Pr[\|\hat{z}_v - z_v\|_2 \geq \varepsilon] \leq \delta$,
- $\hat{\mathcal{O}}_g(v, \varepsilon, \delta)$: an estimate $\widehat{\frac{\partial z_v}{\partial \theta}}$ of $\frac{\partial z_v}{\partial \theta}$ such that $\Pr[\|\widehat{\frac{\partial z_v}{\partial \theta}} - \frac{\partial z_v}{\partial \theta}\|_F \geq \varepsilon] \leq \delta$,

where $\varepsilon > 0$ is the error tolerance, $1 - \delta$ is the confidence probability, and $\|\cdot\|_2$ and $\|\cdot\|_F$ are the Euclidean and Frobenius norm, respectively.

Under the fixed model structure (i.e., the number of layers L , the message passing functions, and the update functions), we construct an algorithm that calculates $\hat{\mathcal{O}}_z$ and $\hat{\mathcal{O}}_g$ in constant time irrespective of the number of the nodes, edges, and neighbors of the input.

However, it is impossible to construct a constant time algorithm without any assumption about the inputs, as shown in Section 5. Therefore, we make the following mild assumptions.

Assumption 1 $\exists B \in \mathbb{R}$ s.t. $\|x_i\|_2 \leq B$, $\|e_{iu}\|_2 \leq B$, and $\|\theta\|_2 \leq B$.

Assumption 2 $\text{deg}(i)M_{liu}$ and U_l are uniformly continuous in any bounded domain.

Assumption 3 (Only for gradient computation) $\text{deg}(i)DM_{liu}$ and DU_l are uniformly continuous in any bounded domain, where D denotes the Jacobian operator.

Intuitively, the first assumption is needed because the absolute error cannot be bounded if the scale of inputs becomes infinitely large. The second and third assumptions are needed to prohibit the amplification of errors in the message passing phase. Furthermore, we derive the query complexity of neighbor sampling when the message functions and update functions satisfy the following assumptions.

Assumption 4 $\exists K \in \mathbb{R}$ s.t. $\text{deg}(i)M_{liu}$ and U_l are K -Lipschitz continuous in any bounded domain.

Assumption 5 (Only for gradient computation) $\exists K' \in \mathbb{R}$ s.t. $\text{deg}(i)DM_{liu}$ and DU_l are K' -Lipschitz continuous in any bounded domain.

4. Main Results

4.1. Constant Time Embedding Approximation

Algorithm 2 $\hat{\mathcal{O}}_z^{(l)}$: Estimate the embedding $z_v^{(l)}$

Require: Graph $G = (\mathcal{V}, \mathcal{E})$ (as oracle); Features $\mathbf{X} \in \mathbb{R}^{n \times d_0}$ (as oracle); Node index $v \in \mathcal{V}$; Model parameters θ ; Error tolerance ε ; Confidence probability $1 - \delta$.

Ensure: Approximation of the embedding $z_v^{(l)}$

- 1: $\mathcal{S}^{(l)} \leftarrow$ sample $r^{(l)}(\varepsilon, \delta)$ neighbors of v with uniform random with replacement.
- 2: $\hat{\mathbf{h}}_v^{(l)} \leftarrow \begin{cases} \frac{\mathcal{O}_{\text{deg}(v)}}{r^{(l)}} \sum_{u \in \mathcal{S}^{(l)}} M_{lvu}(\mathcal{O}_{\text{feature}}(v), \mathcal{O}_{\text{feature}}(u), \mathbf{e}_{iu}, \theta) & (l = 1) \\ \frac{\mathcal{O}_{\text{deg}(v)}}{r^{(l)}} \sum_{u \in \mathcal{S}^{(l)}} M_{lvu}(\hat{\mathcal{O}}_z^{(l-1)}(v \leftarrow v), \hat{\mathcal{O}}_z^{(l-1)}(v \leftarrow u), \mathbf{e}_{iu}, \theta) & (l > 1) \end{cases}$
- 3: $\hat{z}_v^{(l)} \leftarrow U_l(\hat{\mathcal{O}}_z^{(l-1)}(v \leftarrow v), \hat{\mathbf{h}}_v^{(l)}, \theta)$ if $l > 1$ otherwise $U_l(\mathcal{O}_{\text{feature}}(v), \hat{\mathbf{h}}_v^{(l)}, \theta)$
- 4: **return** \hat{z}_i

Now, we describe the construction of a constant time approximation algorithm based on neighbor sampling, which approximates the embedding z_v with an absolute error of at most ε and probability $1 - \delta$. We recursively constructed the algorithm layer by layer by sampling $r^{(l)}$ neighboring nodes in layer l . We refer to the algorithm that calculates the estimate of the embeddings in the l -th layer $z^{(l)}$ as $\hat{\mathcal{O}}_z^{(l)}$ ($l = 1, \dots, L$). Algorithm 2 presents the pseudo code. Here, $\hat{\mathcal{O}}_z^{(l-1)}(v \leftarrow u)$ represents calling the function $\hat{\mathcal{O}}_z^{(l-1)}$ with the same parameters as the current function, except for v , which is replaced by u . In the following, we demonstrate the theoretical properties of Algorithm 2.

Theorem 1. For all $\varepsilon > 0, 1 > \delta > 0$, there exists $r^{(l)}(\varepsilon, \delta)$ ($l = 1, \dots, L$) such that for all inputs satisfying Assumptions 1 and 2, the following property holds true:

$$\Pr[\|\hat{\mathcal{O}}_z(v, \varepsilon, \delta) - z_v\|_2 \geq \varepsilon] \leq \delta.$$

Theorem 1 shows that the approximation error of Algorithm 2 is bounded by ε with probability $1 - \delta$. It is proved by applying Hoeffding's inequality (Hoeffding, 1963) recursively. The complete proof is provided in the appendices. Because the number of sampled nodes depends only on ε and δ and is independent of the number of the nodes, edges, and neighbors of the input, Algorithm 2 operates in constant time. We provide the complexity when the functions are Lipschitz continuous.

Theorem 2. Under Assumptions 1 and 4, $r^{(L)} = O(\frac{1}{\varepsilon^2} \log \frac{1}{\delta})$ and $r^{(1)}, \dots, r^{(L-1)} = O(\frac{1}{\varepsilon^2} (\log \frac{1}{\varepsilon} + \log \frac{1}{\delta}))$ are sufficient, and the query complexity of Algorithms 2 is $O(\frac{1}{\varepsilon^{2L}} (\log \frac{1}{\varepsilon} + \log \frac{1}{\delta})^{L-1} \log \frac{1}{\delta})$.

Although the complexity is exponential with respect to the number of layers, this is nonetheless beneficial, because the number of layers is usually small in practice. For example, the original GCN employs two layers (Kipf & Welling, 2017). It is noteworthy that, although most constant time algorithms proposed in the literature also depend on some parameters exponentially, they have nonetheless been proved to be effective. For example, the constant time algorithms of Yoshida et al. (2009) for the maximum matching prob-

lem and minimum set cover problem use $d^{O(\frac{1}{\varepsilon^2})} (\frac{1}{\varepsilon})^{O(\frac{1}{\varepsilon})}$ and $\frac{1}{\varepsilon^2} (st)^{O(s)}$ queries, respectively, where d is the maximum degree and s is the number of elements in a set, and each element is in at most t sets. The important point here is that the complexity is completely independent of the size of the inputs, which is desirable, especially when the input size is very large. In addition, we show that the query complexity of Algorithm 2 is optimal with respect to ε if the number of layers is one. In other words, a one-layer model cannot be approximated in $o(\frac{1}{\varepsilon^2})$ time by any algorithm.

Theorem 3. Under Assumptions 1 and 4 and $L = 1$, the time complexity of Algorithm 2 in Theorem 2 is optimal with respect to the error tolerance ε .

The proof is based on Chazelle et al.'s lemma (Chazelle et al., 2005). The optimality when $L \geq 2$ is an open problem.

4.2. Constant Time Gradient Approximation

Now, we show that the neighbor sampling technique can guarantee the approximation errors of the gradient of embeddings with respect to the model parameters. Let $\frac{\partial z_v}{\partial \theta}$ be the gradient of the embedding z_v with respect to the model parameter θ , i.e., $(\frac{\partial z_v}{\partial \theta})_{ijk} = \frac{\partial z_{vi}}{\partial \theta_{jk}}$.

Theorem 4. For all $\varepsilon > 0, 1 > \delta > 0$, there exists $r^{(l)}(\varepsilon, \delta)$ ($l = 1, \dots, L$) such that for all inputs satisfying Assumptions 1, 2, and 3, the following property holds true:

$$\Pr[\|\widehat{\frac{\partial z_v^{(L)}}{\partial \theta}} - \frac{\partial z_v^{(L)}}{\partial \theta}\|_F \geq \varepsilon] \leq \delta,$$

where $\widehat{\frac{\partial z_v^{(L)}}{\partial \theta}}$ is the gradient of $\hat{z}_v^{(L)}$, which is obtained by $\hat{\mathcal{O}}_z^{(L)}(v, \varepsilon, \delta)$, with respect to θ .

Therefore, an estimate of the gradient of the embedding with respect to parameters with an absolute error of at most ε and probability $1 - \delta$ can be calculated by running $\hat{\mathcal{O}}_z^{(L)}(v, \varepsilon, \delta)$ and calculating the gradient of the obtained estimate of the embedding. We provide the complexity when the functions are Lipschitz continuous.

Theorem 5. Under Assumptions 1, 4, and 5, $r^{(L)} = O(\frac{1}{\varepsilon^2} \log \frac{1}{\delta})$ and $r^{(1)}, \dots, r^{(L-1)} = O(\frac{1}{\varepsilon^2} (\log \frac{1}{\varepsilon} + \log \frac{1}{\delta}))$ are sufficient, and the gradient of the embedding with respect to parameters can be approximated with an absolute error of at most ε and probability $1 - \delta$ in $O(\frac{1}{\varepsilon^2 L} (\log \frac{1}{\varepsilon} + \log \frac{1}{\delta})^{L-1} \log \frac{1}{\delta})$ time.

Note that, technically, MPNNs do not include GATs, because these networks use embeddings of other neighboring nodes to calculate the attention value. However, Theorems 1 and 4 can be naturally extended to GATs, and we can approximate GATs in constant time by neighbor sampling. This is surprising, because GATs may pay considerable attention to some nodes, and uniform sampling may fail to sample these nodes. However, it can be shown that our assumptions, which do not seem related to this issue, prohibit this situation. The details are described in the appendices.

5. Inapproximability

In this section, we show that some existing GNNs cannot be approximated in constant time. The theorems state that these models cannot be approximated in constant time by either neighbor sampling or *any other algorithm*. In other words, for any algorithm that operates in constant time, there exists an error tolerance ε , a confidence probability $1 - \delta$, and a counter example input such that the approximation error for the input is more than ε with probability δ . This indicates that the application of an approximation method to these models requires close supervision, because the obtained embedding may be significantly different from the exact embedding.

Proposition 6. If $\|x_i\|_2$ or $\|\theta\|_F$ is not bounded, even under Assumption 2, the embeddings of GraphSAGE-GCN cannot be approximated with arbitrary precision and probability in constant time.

Proposition 6 indicates that Assumption 1 is necessary for constant-time approximation.

Proposition 7. Even under Assumption 1, the embeddings and gradients of GraphSAGE-GCN with ReLU activation and normalization cannot be approximated with arbitrary precision and probability in constant time.

In other words, Proposition 7 shows that the original model of GraphSAGE-GCN cannot be approximated within constant time. We confirm this fact through computational experiments in Section 6 (Q2).

Proposition 8. Even under Assumptions 1 and 2, the gradients of GraphSAGE-GCN with ReLU activation cannot be approximated with arbitrary precision and probability in constant time.

This indicates that the activation function is important for constant-time approximability, because the gradient of

GraphSAGE-GCN with sigmoid activation can be approximated within constant time by neighbor sampling (Theorem 4). We confirm this fact through computational experiments in Section 6 (Q3). The following two theorems state that GraphSAGE-pool and GCN cannot be approximated in constant time even under Assumptions 1, 2, and 3.

Proposition 9. Even under Assumptions 1, 2, and 3, the embeddings of GraphSAGE-pool cannot be approximated with arbitrary precision and probability in constant time.

Proposition 10. Even under Assumptions 1, 2, and 3, the embeddings of GCN cannot be approximated with arbitrary precision and probability in constant time.

Constant Time Approximation for GCNs: Because of the inapproximability theorems, GCNs cannot be approximated in constant time. However, GCNs can be approximated in constant time if the input graph satisfies the following property.

Assumption 6 There exists a constant $C \in \mathbb{R}$ such that, for any input graph $G = (\mathcal{V}, \mathcal{E})$ and node $v, u \in \mathcal{V}$, the ratio of $\deg(v)$ to $\deg(u)$ is at most C (i.e., $\deg(v)/\deg(u) \leq C$).

Assumption 6 prohibits input graphs that have a skewed degree distribution. GCNs require Assumption 6, because the norm of the embedding is not bounded and the influence of anomaly nodes with low degrees is significant without it. It should be noted that the GraphSAGE-pool cannot be approximated in constant time even under Assumption 6. We confirm this fact through computational experiments in Section 6 (Q5).

These negative results reveal which information each GNN model gives importance to in the light of the computational complexity. For example, GCNs cannot be approximated in constant time when a high-degree node that neighbors anomaly low-degree nodes exists in the input graph, and GCNs requires the information of anomaly nodes in addition to majority nodes to be approximated accurately. This indicates that the exact computation of GCNs gives importance to these anomaly nodes as well as majority nodes. In contrast, GraphSAGE-GCN ignores these anomaly nodes and takes only majority nodes into account even in the exact computation. This is why GraphSAGE-GCN can be approximated accurately only with a constant number of samples. This observation suggests that GCNs should be used when the anomaly nodes play important roles in the problem considered, and otherwise GraphSAGE-GCN should be used, because GraphSAGE-GCN can infer faster than GCNs by neighbor sampling. This type of observation can be applied to other models such as GraphSAGE-pool and GATs as well.

6. Experiments

In this study, we focused on validating our theoretical results through numerical experiments, because Hamilton et al. (2017) have already reported the effect of neighbor sampling for downstream machine learning tasks (e.g., classification). Namely, we answer the following questions through experiments.

- Q1:** How fast is the constant time approximation algorithm (Algorithm 2)?
- Q2:** Does neighbor sampling (Algorithm 2) accurately approximate the embeddings of GraphSAGE-GCN without normalization (Theorem 1), whereas it cannot approximate the original one (Proposition 7)?
- Q3:** Does neighbor sampling (Algorithm 2) accurately approximate the gradients of GraphSAGE-GCN with sigmoid activation (Theorem 4), whereas it cannot approximate that with ReLU activation (Proposition 8)?
- Q4:** Is the theoretical rate of the approximation error of Algorithm 2 tight?
- Q5:** Does neighbor sampling fail to approximate GCNs when the degree distribution is skewed (Proposition 10)? Does it succeed when the node distribution is flat (Assumption 6)?
- Q6:** Does neighbor sampling work efficiently for real data?

The experimental details are described in the appendices.

Experiments for Q1: We measured the speed of exact computation and the neighbor sampling of two-layer GraphSAGE-GCN and two-layer GATs. We initialized parameters using the i.i.d. standard multivariate normal distribution. The input graph was a clique K_n . We used ten-dimensional vectors from the i.i.d. standard multivariate normal distribution as the node features. We took $r^{(1)} = r^{(2)} = 100$ samples. For each method and $n = 2^7, 2^8, \dots, 2^{19}$, we ran inference 10 times and measured the average time consumption and standard deviation. Figure 1 (a) plots the speed of these methods as the number of nodes increases. This shows that the neighbor sampling is several orders of magnitude faster than the exact computation when the graph size is extremely large.

Experiments for Q2: We used the original one-layer GraphSAGE-GCN (with ReLU activation and normalization) and one-layer GraphSAGE-GCN with ReLU activation. The input graph was a clique K_n , the features of which were $\mathbf{x}_1 = (1, 0)^\top$ and $\mathbf{x}_i = (0, 1/n)^\top$ ($i \neq 1$), and the weight matrix was an identity matrix \mathbf{I}_2 . We used $r^{(1)} = 5, 30$, and 100 as the sample size. If a model can

be approximated in constant time, the approximation error goes to zero as the sample size increases, even if the graph size reaches infinity. The approximation errors of both models are illustrated in Figure 1 (b). The approximation error of the original GraphSAGE-GCN converges to approximately 0.75 even if the sample size increases. In contrast, the approximation error without normalization becomes increasingly bounded as the sample size increases. This is consistent with Theorems 1 and 7.

Experiments for Q3: We examined the approximation errors of the gradients using the one-layer GraphSAGE-GCN with ReLU activation and sigmoid activation. The input graph was a clique K_n , the features of which were $\mathbf{x}_1 = (1, 2)^\top$ and $\mathbf{x}_i = (1, 1)^\top$ ($i \neq 1$), and the weight matrix was $((-1, 1))$. We used $r^{(1)} = 5, 30$, and 100 as the sample size. Figure 1 (c) illustrates the approximation error of both models. The approximation error with ReLU activation converges to approximately 1.0, even if the sample size increases. In contrast, the approximation error with sigmoid activation becomes increasingly bounded as the sample size increases. This is consistent with Theorems 4 and 8.

Experiments for Q4: We used one-layer GraphSAGE-GCN with sigmoid activation. The input graph was a clique K_n with $n = 40000$ nodes. We set the dimensions of intermediate embeddings as 2, and each feature value was set to 1 with probability 0.5 and -1 otherwise. This satisfies Assumption 1, i.e., $\|\mathbf{x}_i\|_2 \leq \sqrt{2}$. We computed the approximation errors of Algorithm 2 with different numbers of samples. Figure 1 (d) illustrates the 99-th percentile point of empirical approximation errors and the theoretical bound by Theorem 2, i.e., $\varepsilon = O(r^{-1/2})$. It shows that the approximation error decreases together with the theoretical rate. This indicates that the theoretical rate is tight.

Experiments for Q5: We analyzed the instances when neighbor sampling succeeds and fails for a variety of models. First, we used the Barabasi–Albert model (BA model) (Barabasi & Albert, 1999) to generate input graphs. The degree distribution of the BA model follows a power law, which indicates neighbor sampling will fail to approximate GCNs (Proposition 10, Assumption 6). We used two-layer GraphSAGE-GCN, GATs, and GCNs with ReLU activation. We used ten-dimensional vectors from the i.i.d. standard multivariate normal distribution as the node features. We used the same number r of samples in the first and second layer, i.e., $r = r^{(1)} = r^{(2)}$, and we changed the value of r from 8 to 1000. We used graphs with $n = r^2$ nodes. Note that if constant time approximation is possible, the error is bounded as the number of samples increases even if the number of nodes increases. Figure 1 (e) shows that the error of GCNs linearly increases, even if the number of samples increases. However, the errors of GraphSAGE-

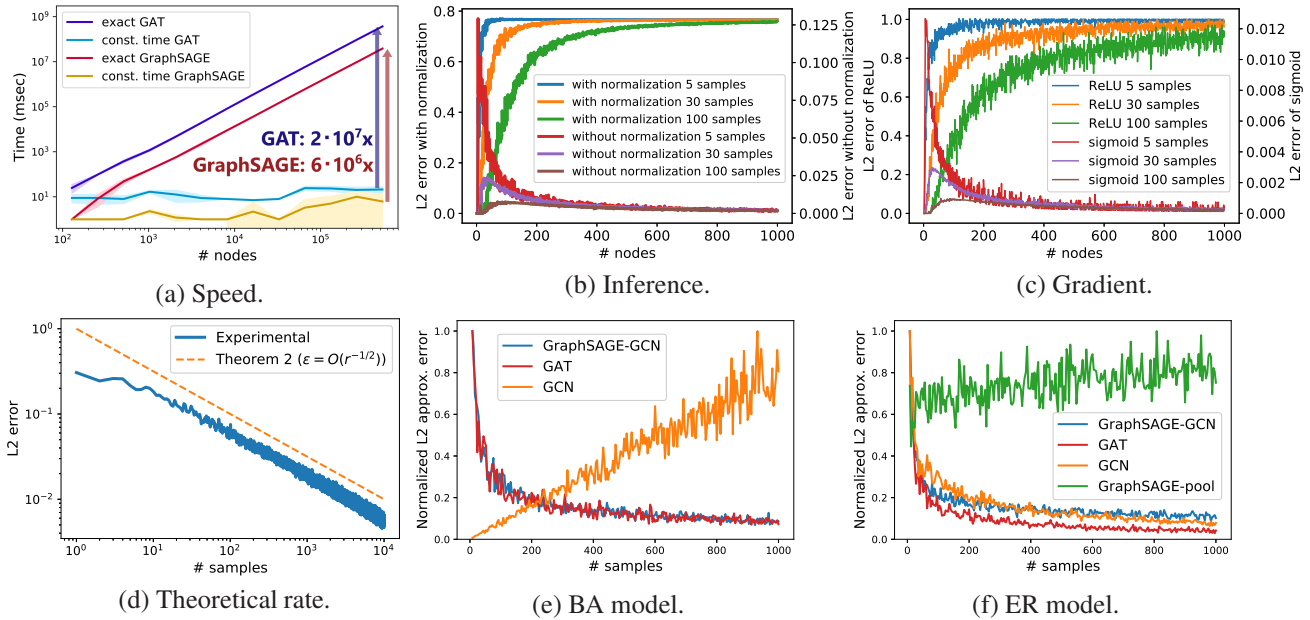


Figure 1. (a) Inference speed of each method. (b) Approximation error of the original GraphSAGE-GCN (i.e., with ReLU activation and normalization) and GraphSAGE-GCN with ReLU activation. (c) Approximation error of the gradient with ReLU and sigmoid activations. (d) Approximation error of Algorithm 2 and its theoretical bound. (e) Approximation error of GraphSAGE-GCN, GATs, and GCNs with the Barabasi–Albert model. (f) Approximation error of GraphSAGE-GCN, GATs, GCNs, and GraphSAGE-pool with the Erdős–Rényi model.

GCN and GATs gradually decrease as the number of samples increases. This indicates that we cannot bound the approximation error of GCNs however the large number of examples we use. This is consistent with Proposition 10. This result indicates that the approximation of GCNs requires close supervision when the input graph is a social network, because the degree distribution of a social network presents the power law as the BA model.

Next, we used the Erdős–Rényi model (ER model) (Erdős & Rényi, 1959). It generates graphs with flat degree distribution. We used the two-layer GraphSAGE-GCN, GATs, GCNs, and GraphSAGE-pool. Figure 1 (f) shows the approximation error. It shows that the errors of GraphSAGE-GCN, GATs, and GCNs gradually decrease as the number of samples increases. This is consistent with Theorem 1 and Assumption 6. In contrast, the approximation error of GraphSAGE-pool does not decrease, even if the input graphs are generated by the ER model. This is consistent with Proposition 9.

Experiments for Q6:

We used three real-world datasets: Cora, PubMed, and Reddit. They contain 2708, 19717, and 232965 nodes, respectively. We randomly chose 500 nodes for validation and

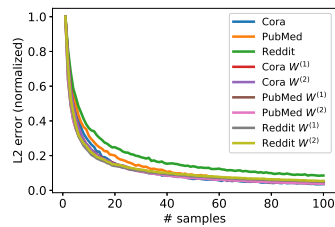


Figure 2. Real data.

1000 nodes for testing and use the remaining nodes for training. We used two-layer GraphSAGE-GCN with sigmoid activation in this experiment. The dimensions of the hidden layers were set to 128, and we used an additional fully connected layer to predict the labels of the nodes from the embeddings. We trained the models with Adam (Kingma & Ba, 2015) with a learning rate of 0.001. We first trained ten models with training nodes for each dataset. The micro-F1 scores of Cora, PubMed, and Reddit were 0.877, 0.839, and 0.901, respectively. It should be noted that we did not aim to obtain high classification accuracy in this experiment but intended only to sanity check the models. In this experiment, we used the same number r of samples in the first and second layer to compute the embeddings of test nodes, i.e., $r = r^{(1)} = r^{(2)}$, and changed the value of r from 1 to 100. We also calculated the gradient of parameter matrices $\mathbf{W}^{(1)}$ and $\mathbf{W}^{(2)}$ with respect to the embedding obtained by Algorithm 2. We compared these values with exact embeddings and exact gradients. Figure 6 illustrates the 99-th percentile point of the empirical approximation errors. We normalized them to ensure that the value was 1.0 at $r = 1$ to demonstrate the decreasing rate. The figure shows that the approximation errors of embeddings and gradients rapidly decrease for the real-world data.

7. Conclusion

We analyzed neighbor sampling to prove that it can approximate the embedding and gradient of GNNs in constant time, where the complexity is completely independent of the number of the nodes, edges, and neighbors of the input. This is the first analysis that offers constant time approximation for GNNs. We further demonstrated that some existing GNNs cannot be approximated in constant time by any algorithm. Finally, we validated the theory through experiments using synthetic and real-world datasets.

8. Acknowledgments

This work was supported by JSPS KAKENHI Grant-Number 15H01704 and the JST PRESTO program JP-MJPR165A.

References

- Angluin, D. Local and global properties in networks of processors (extended abstract). In *Proceedings of the 12th Annual ACM Symposium on Theory of Computing, STOC*, pp. 82–93, 1980.
- Barabasi, A.-L. and Albert, R. Emergence of scaling in random networks. *Science*, 286(5439):509–512, 1999.
- Baskin, I. I., Palyulin, V. A., and Zefirov, N. S. A neural device for searching direct correlations between structures and properties of chemical compounds. *Journal of Chemical Information and Computer Sciences*, 37(4): 715–721, 1997.
- Bruna, J., Zaremba, W., Szlam, A., and LeCun, Y. Spectral networks and locally connected networks on graphs. In *2nd International Conference on Learning Representations, ICLR*, 2014.
- Chazelle, B., Rubinfeld, R., and Trevisan, L. Approximating the minimum spanning tree weight in sublinear time. *SIAM J. Comput.*, 34(6):1370–1379, 2005.
- Chen, J., Ma, T., and Xiao, C. FastGCN: Fast learning with graph convolutional networks via importance sampling. In *Proceedings of the Sixth International Conference on Learning Representations, ICLR*, 2018a.
- Chen, J., Zhu, J., and Song, L. Stochastic training of graph convolutional networks with variance reduction. In *Proceedings of the 35th International Conference on Machine Learning, ICML*, pp. 941–949, 2018b.
- Chiang, W., Liu, X., Si, S., Li, Y., Bengio, S., and Hsieh, C. Cluster-gcn: An efficient algorithm for training deep and large graph convolutional networks. In *Proceedings of the 25th ACM SIGKDD International Conference on Knowledge Discovery & Data Mining, KDD*, pp. 257–266, 2019.
- Czumaj, A. and Sohler, C. Estimating the weight of metric minimum spanning trees in sublinear-time. In *Proceedings of the 36th Annual ACM Symposium on Theory of Computing, STOC*, pp. 175–183, 2004.
- Defferrard, M., Bresson, X., and Vandergheynst, P. Convolutional neural networks on graphs with fast localized spectral filtering. In *Advances in Neural Information Processing Systems 29, NIPS*, pp. 3837–3845, 2016.
- Duvenaud, D., Maclaurin, D., Aguilera-Iparraguirre, J., Gómez-Bombarelli, R., Hirzel, T., Aspuru-Guzik, A., and Adams, R. P. Convolutional networks on graphs for learning molecular fingerprints. In *Advances in Neural Information Processing Systems 28, NIPS*, pp. 2224–2232, 2015.
- Erdős, P. and Rényi, A. On random graphs I. *Publicationes Mathematicae*, 6:290–297, 1959.
- Fan, W., Ma, Y., Li, Q., He, Y., Zhao, Y. E., Tang, J., and Yin, D. Graph neural networks for social recommendation. In *The World Wide Web Conference, WWW*, pp. 417–426, 2019.
- Gilmer, J., Schoenholz, S. S., Riley, P. F., Vinyals, O., and Dahl, G. E. Neural message passing for quantum chemistry. In *Proceedings of the 34th International Conference on Machine Learning, ICML*, pp. 1263–1272, 2017.
- Glorot, X. and Bengio, Y. Understanding the difficulty of training deep feedforward neural networks. In *Proceedings of the Thirteenth International Conference on Artificial Intelligence and Statistics, AISTATS*, pp. 249–256, 2010.
- Gori, M., Monfardini, G., and Scarselli, F. A new model for learning in graph domains. In *Proceedings of the International Joint Conference on Neural Networks, IJCNN*, volume 2, pp. 729–734, 2005.
- Hamilton, W. L., Ying, Z., and Leskovec, J. Inductive representation learning on large graphs. In *Advances in Neural Information Processing Systems 30, NIPS*, pp. 1025–1035, 2017.
- Hayashi, K. and Yoshida, Y. Minimizing quadratic functions in constant time. In *Advances in Neural Information Processing Systems 29, NIPS*, pp. 2217–2225, 2016.
- Hayashi, K. and Yoshida, Y. Fitting low-rank tensors in constant time. In *Advances in Neural Information Processing Systems 30, NIPS*, pp. 2470–2478, 2017.

- Hoeffding, W. Probability inequalities for sums of bounded random variables. *Journal of the American Statistical Association*, 58(301):13–30, March 1963.
- Huang, W., Zhang, T., Rong, Y., and Huang, J. Adaptive sampling towards fast graph representation learning. In *Advances in Neural Information Processing Systems 31, NeurIPS*, 2018.
- Indyk, P. A sublinear time approximation scheme for clustering in metric spaces. In *Proceedings of the 40th Annual Symposium on Foundations of Computer Science, FOCS*, pp. 154–159, 1999.
- Kingma, D. P. and Ba, J. Adam: A method for stochastic optimization. In *Proceedings of the Third International Conference on Learning Representations, ICLR*, 2015.
- Kipf, T. N. and Welling, M. Semi-supervised classification with graph convolutional networks. In *Proceedings of the Fifth International Conference on Learning Representations, ICLR*, 2017.
- Li, Y., Tarlow, D., Brockschmidt, M., and Zemel, R. S. Gated graph sequence neural networks. In *4th International Conference on Learning Representations, ICLR*, 2016.
- Merkwirth, C. and Lengauer, T. Automatic generation of complementary descriptors with molecular graph networks. *Journal of Chemical Information and Modeling*, 45(5):1159–1168, 2005.
- Mishra, N., Oblinger, D., and Pitt, L. Sublinear time approximate clustering. In *Proceedings of the Twelfth Annual Symposium on Discrete Algorithms, SODA*, pp. 439–447, 2001.
- Morris, C., Ritzert, M., Fey, M., Hamilton, W. L., Lenssen, J. E., Rattan, G., and Grohe, M. Weisfeiler and leman go neural: Higher-order graph neural networks. In *The Thirty-Third AAAI Conference on Artificial Intelligence, AAAI*, pp. 4602–4609, 2019.
- Nguyen, H. N. and Onak, K. Constant-time approximation algorithms via local improvements. In *Proceedings of the 49th Annual IEEE Symposium on Foundations of Computer Science, FOCS*, pp. 327–336, 2008.
- Park, N., Kan, A., Dong, X. L., Zhao, T., and Faloutsos, C. Estimating node importance in knowledge graphs using graph neural networks. In *Proceedings of the 25th ACM SIGKDD International Conference on Knowledge Discovery & Data Mining, KDD*, pp. 596–606, 2019.
- Parnas, M. and Ron, D. Approximating the minimum vertex cover in sublinear time and a connection to distributed algorithms. *Theor. Comput. Sci.*, 381(1-3):183–196, 2007.
- Rubinfeld, R. and Sudan, M. Robust characterizations of polynomials with applications to program testing. *SIAM J. Comput.*, 25(2):252–271, 1996.
- Sato, R., Yamada, M., and Kashima, H. Approximation ratios of graph neural networks for combinatorial problems. In *Advances in Neural Information Processing Systems 32, NeurIPS*, 2019.
- Scarselli, F., Gori, M., Tsoi, A. C., Hagenbuchner, M., and Monfardini, G. The graph neural network model. *IEEE Trans. Neural Networks*, 20(1):61–80, 2009.
- Schlichtkrull, M. S., Kipf, T. N., Bloem, P., van den Berg, R., Titov, I., and Welling, M. Modeling relational data with graph convolutional networks. In *The Semantic Web - 15th International Conference, ESWC*, pp. 593–607, 2018.
- Sperduti, A. and Starita, A. Supervised neural networks for the classification of structures. *IEEE Trans. Neural Networks*, 8(3):714–735, 1997.
- Suomela, J. Survey of local algorithms. *ACM Comput. Surv.*, 45(2):24:1–24:40, 2013.
- Veličković, P., Cucurull, G., Casanova, A., Romero, A., Liò, P., and Bengio, Y. Graph attention networks. In *Proceedings of the Sixth International Conference on Learning Representations, ICLR*, 2018.
- Wang, H., Zhao, M., Xie, X., Li, W., and Guo, M. Knowledge graph convolutional networks for recommender systems. In *The World Wide Web Conference, WWW*, pp. 3307–3313, 2019a.
- Wang, X., He, X., Cao, Y., Liu, M., and Chua, T. KGAT: knowledge graph attention network for recommendation. In *Proceedings of the 25th ACM SIGKDD International Conference on Knowledge Discovery & Data Mining, KDD*, pp. 950–958, 2019b.
- Weisfeiler, B. and Lehman, A. A. A reduction of a graph to a canonical form and an algebra arising during this reduction. *Nauchno-Technicheskaya Informatsia*, 2(9): 12–16, 1968.
- Xu, K., Hu, W., Leskovec, J., and Jegelka, S. How powerful are graph neural networks? In *7th International Conference on Learning Representations, ICLR*, 2019.
- Ying, R., He, R., Chen, K., Eksombatchai, P., Hamilton, W. L., and Leskovec, J. Graph convolutional neural networks for web-scale recommender systems. In *Proceedings of the 24th ACM SIGKDD International Conference on Knowledge Discovery & Data Mining, KDD*, pp. 974–983, 2018.

- Yoshida, Y., Yamamoto, M., and Ito, H. An improved constant-time approximation algorithm for maximum matchings. In *Proceedings of the 41st Annual ACM Symposium on Theory of Computing, STOC*, pp. 225–234, 2009.
- Zhang, M., Cui, Z., Neumann, M., and Chen, Y. An end-to-end deep learning architecture for graph classification. In *Proceedings of the Thirty-Second AAAI Conference on Artificial Intelligence, AAAI*, pp. 4438–4445, 2018.
- Zou, D., Hu, Z., Wang, Y., Jiang, S., Sun, Y., and Gu, Q. Layer-dependent importance sampling for training deep and large graph convolutional networks. In *Advances in Neural Information Processing Systems 32, NeurIPS*, pp. 11247–11256, 2019.

A. Models

We introduce GraphSAGE-GCN, GraphSAGE-mean, GraphSAGE-pool, the graph convolutional networks (GCNs), and the graph attention networks (GATs) for completeness of our paper.

GraphSAGE-GCN (Hamilton et al., 2017): The message function and the update function of this model is

$$M_{lvu}(\mathbf{z}_v, \mathbf{z}_u, e_{vu}, \boldsymbol{\theta}) = \frac{\mathbf{z}_u}{\deg(v)},$$

$$U_l(\mathbf{z}_v, \mathbf{h}_v, \boldsymbol{\theta}) = \sigma(\mathbf{W}^{(l)} \mathbf{h}_v),$$

where $\mathbf{W}^{(l)}$ is a parameter matrix and σ is an activation function such as sigmoid and ReLU. GraphSAGE-GCN includes the center node itself in the set of adjacent nodes (i.e., $\mathcal{N}(v) \leftarrow \mathcal{N}(v) \cup \{v\}$).

GraphSAGE-mean (Hamilton et al., 2017): The message function and the update function of this model is

$$M_{lvu}(\mathbf{z}_v, \mathbf{z}_u, e_{vu}, \boldsymbol{\theta}) = \frac{\mathbf{z}_v}{\deg(v)},$$

$$U_l(\mathbf{z}_v, \mathbf{h}_v, \boldsymbol{\theta}) = \sigma(\mathbf{W}^{(l)} [\mathbf{z}_v, \mathbf{h}_v]),$$

where $[\cdot]$ denotes concatenation.

GraphSAGE-pool (Hamilton et al., 2017): We do not formulate GraphSAGE-pool using the message function and the update function because it takes maximum instead of summation. The model of GraphSAGE-pool is

$$\mathbf{z}_v^{(l)} = \max(\{\sigma(\mathbf{W}^{(l)} \mathbf{z}_u^{(l-1)} + \mathbf{b}) \mid u \in \mathcal{N}(v)\}).$$

GCNs (Kipf & Welling, 2017): The message function and the update function of this model is

$$M_{lvu}(\mathbf{z}_v, \mathbf{z}_u, e_{vu}, \boldsymbol{\theta}) = \frac{\mathbf{z}_u}{\sqrt{\deg(v)\deg(u)}},$$

$$U_l(\mathbf{z}_v, \mathbf{h}_v, \boldsymbol{\theta}) = \sigma(\mathbf{W}^{(l)} \mathbf{h}_v).$$

GATs (Veličković et al., 2018): The message function and the update function of this model is

$$\alpha_{vu}^{(l)} = \frac{\exp(\text{LEAKYRELU}(\mathbf{a}^{(l)\top} [\mathbf{W}^{(l)} \mathbf{z}_v, \mathbf{W}^{(l)} \mathbf{z}_u]))}{\sum_{u' \in \mathcal{N}(v)} \exp(\text{LEAKYRELU}(\mathbf{a}^{(l)\top} [\mathbf{W}^{(l)} \mathbf{z}_v, \mathbf{W}^{(l)} \mathbf{z}_{u'}]))},$$

$$M_{lvu}(\mathbf{z}_v, \mathbf{z}_u, e_{vu}, \boldsymbol{\theta}) = \alpha_{vu}^{(l)} \mathbf{z}_u,$$

$$U_l(\mathbf{z}_v, \mathbf{h}_v, \boldsymbol{\theta}) = \sigma(\mathbf{W}^{(l)} \mathbf{h}_v).$$

Note that, technically, MPNNs do not include GATs because GATs use embeddings of other neighboring nodes to calculate the attention value α_{vu} . However, we can apply the same argument as MPNNs to GATs, and neighbor sampling can approximate GATs in constant time as other MPNNs. To be precise, the following proposition holds true.

Proposition 11. *If Assumptions 1 holds true and σ is Lipschitz continuous, if we take $r^{(L)} = O(\frac{1}{\varepsilon^2} \log \frac{1}{\delta})$ and*

$r^{(1)}, \dots, r^{(L-1)} = O(\frac{1}{\varepsilon^2}(\log \frac{1}{\varepsilon} + \log \frac{1}{\delta}))$ samples, and let

$$\begin{aligned}\hat{\mathbf{z}}_v^{(0)} &= \mathbf{z}_v^{(0)} \\ \hat{\alpha}_{vu}^{(l)} &= \frac{\exp(\text{LEAKYRELU}(\mathbf{a}^{(l)\top}[\mathbf{W}^{(l)}\hat{\mathbf{z}}_v^{(l-1)}, \mathbf{W}^{(l)}\hat{\mathbf{z}}_u^{(l-1)}]))}{\sum_{u' \in \mathcal{S}^{(l)}} \exp(\text{LEAKYRELU}(\mathbf{a}^{(l)\top}[\mathbf{W}^{(l)}\hat{\mathbf{z}}_v^{(l-1)}, \mathbf{W}^{(l)}\hat{\mathbf{z}}_{u'}^{(l-1)}]))}, \\ \hat{\mathbf{h}}_v^{(l)} &= \sum_{u \in \mathcal{S}^{(l)}} \hat{\alpha}_{vu}^{(l)} \hat{\mathbf{z}}_u^{(l-1)}, \\ \hat{\mathbf{z}}_v^{(l)} &= U_l(\hat{\mathbf{z}}_v^{(l-1)}, \hat{\mathbf{h}}_v^{(l)}, \boldsymbol{\theta}).\end{aligned}$$

Then, the following property holds true.

$$\Pr[\|\mathbf{z}_v^{(L)} - \hat{\mathbf{z}}_v^{(L)}\|_2 \geq \varepsilon] < \delta.$$

We prove Proposition 11 in Section C.

B. Experimental Setup

Experiments for Q1:

The speed is evaluated by Intel Xeon CPU E5-2690.

Experiments for Q4: We initialized the weight matrix $\mathbf{W}^{(1)}$ with normal distribution and then normalized it so that the operator norm $\|\mathbf{W}^{(1)}\|_{\text{op}}$ of the matrix was equal to 1. This satisfies Assumption 1, i.e., $\|\boldsymbol{\theta}\|_2 \leq \sqrt{2}$. For each $r = 1, \dots, 10000$, we (1) initialized the weight matrix, (2) choose 400 nodes, (3) calculated the exact embedding of each chosen node, (4) calculated the estimate for each chosen node with r samples, i.e., $r^{(1)} = r$, and (5) calculated the approximation error of each chosen node.

Experiments for Q5: In the experiment for the BA model, we (1) iterated r from 8 to 1000, (2) set $n = r^2$, (3) generated 10 graphs with n nodes using the BA model, (4) chose the node that has the maximum degree for each generated graph, (5) calculated the exact embeddings and its estimate for each chosen node with r samples, i.e., $r^{(1)} = r^{(2)} = r$, and (6) calculated the approximation error.

The experimental process for the ER model was similar to that for the ER model, but we used the ER model instead of BA model and set $n = \text{floor}(r^{1.5})$ instead of $n = r^2$ to reduce the computational cost.

Experiments for Q6: To calculate the approximation errors of embeddings, for each trained model, for $r = 1 \dots 100$, we (1) calculated the exact embedding of each test node, (2) calculated an estimate of embedding of each test node with r samples, i.e., $r^{(1)} = r^{(2)} = r$, and (3) calculated the approximation error of each test node. To calculate the approximation errors of gradients, for each dataset, we (1) initialized ten models with Xavier initializer (Glorot & Bengio, 2010), (2) chose random 1000 training nodes, and (3) for each model, for each chosen node, and for $r = 1 \dots 100$, calculated the exact and approximation gradients of the classification loss with respect to the parameters, and we calculated their approximation error.

C. Proofs

We introduce the following multivariate version of the Hoeffding's inequality (Hoeffding, 1963) to prove the theoretical bound (Theorem 1 and 4).

Lemma 12 (multivariate Hoeffding's inequality). *Let $\mathbf{x}_1, \mathbf{x}_2, \dots, \mathbf{x}_n$ be independent d -dimensional random variables whose two-norms are bounded $\|\mathbf{x}_i\|_2 \leq B$, and let $\bar{\mathbf{x}}$ be the empirical mean of these variables $\bar{\mathbf{x}} = \frac{1}{n} \sum_{i=1}^n \mathbf{x}_i$. Then, for any $\varepsilon > 0$,*

$$\Pr[\|\bar{\mathbf{x}} - \mathbb{E}[\bar{\mathbf{x}}]\|_2 \geq \varepsilon] \leq 2d \exp\left(-\frac{n\varepsilon^2}{2B^2d}\right)$$

holds true.

Lemma 12 states that the empirical mean of $n = O(\frac{1}{\varepsilon^2} \log \frac{1}{\delta})$ samples independently sampled from the same distribution is the approximation of the exact mean with an absolute error of at most ε and probability $1 - \delta$.

Lemma 13 (Hoeffding's inequality (Hoeffding, 1963)). *Let X_1, X_2, \dots, X_n be independent random variables bounded by the intervals $[-B, B]$ and let \bar{X} be the empirical mean of these variables $\bar{X} = \frac{1}{n} \sum_{i=1}^n X_i$. Then, for any $\varepsilon > 0$,*

$$\Pr[|\bar{X} - \mathbb{E}[\bar{X}]| \geq \varepsilon] \leq 2 \exp\left(-\frac{n\varepsilon^2}{2B^2}\right)$$

holds true.

Proof of Lemma 12. Apply Lemma 13 to each dimension k of X_i . Then,

$$\Pr[|\bar{X}_k - \mathbb{E}[\bar{X}]_k| \geq \frac{\varepsilon}{\sqrt{d}}] \leq 2 \exp\left(-\frac{n\varepsilon^2}{2B^2d}\right).$$

It should be noted that $|X_{ik}| < B$ because $\|X_i\|_2 < B$. Therefore,

$$\Pr[\exists k \in \{1, 2, \dots, d\} \mid \bar{X}_k - \mathbb{E}[\bar{X}]_k| \geq \frac{\varepsilon}{\sqrt{d}}] \leq 2d \exp\left(-\frac{n\varepsilon^2}{2B^2d}\right).$$

If $|\bar{X}_k - \mathbb{E}[\bar{X}]_k| < \frac{\varepsilon}{\sqrt{d}}$ holds true for all dimension k , then

$$\|\bar{X} - \mathbb{E}[\bar{X}]\|_2 = \sqrt{\sum_{k=1}^d (\bar{X}_k - \mathbb{E}[\bar{X}]_k)^2} < \sqrt{d \cdot \frac{\varepsilon^2}{d}} = \varepsilon.$$

Therefore,

$$\Pr[\|\bar{X} - \mathbb{E}[\bar{X}]\|_2 \geq \varepsilon] \leq 2d \exp\left(-\frac{n\varepsilon^2}{2B^2d}\right).$$

□

First, we prove that the embedding in each layer is bounded.

Lemma 14. *Under Assumptions 1 and 2, the norms of the embeddings $\|z_v^{(l)}\|_2$, $\|\hat{z}_v^{(l)}\|_2$, $\|h_v^{(l)}\|_2$, and $\|\hat{h}_v^{(l)}\|_2$ ($l = 1, \dots, L$) are bounded by a constant $B \in \mathbb{R}$.*

Proof of Lemma 14. We prove the theorem by performing mathematical induction. The norm of the input to the first layer is bounded by Assumption 1. The message function $\text{deg}(i)M_{liv}$ and the update function U_l is continuous by Assumption 2. Since the image $f(X)$ of a compact set $X \in \mathbb{R}^d$ is compact if f is continuous, the images of $\text{deg}(i)M_{liv}$ and U_l are bounded by induction. □

Proof of Theorem 1. We prove the theorem by performing mathematical induction on the number of layers L .

Base case: It is shown that the statement holds true for $L = 1$.

Because U_L is uniform continuous,

$$\exists \varepsilon' > 0, \forall z_v, h_v, h'_v, \theta, \|h_v - h'_v\|_2 < \varepsilon' \Rightarrow \|U_L(z_v, h_v, \theta) - U_L(z_v, h'_v, \theta)\|_2 < \varepsilon. \quad (1)$$

Let x_k be the k -th sample in $\mathcal{S}^{(L)}$ and $X_k = \text{deg}(v)M_{Lvu}(z_v^{(0)}, z_{x_k}^{(0)}, e_{vx_k}, \theta)$. Then,

$$\mathbb{E}[X_k] = \sum_{u \in \mathcal{N}(v)} M_{Lvu}(z_v^{(0)}, z_u^{(0)}, e_{vu}, \theta) = h_v^{(L)}. \quad (2)$$

There exists a constant $C \in \mathbb{R}$ such that for any input satisfying Assumption 1,

$$\|X_k\|_2 < C \quad (3)$$

holds true because $\|\mathbf{z}_v^{(0)}\|_2, \|\mathbf{z}_{x_k}^{(0)}\|_2, \|\mathbf{e}_{vx_k}\|_2$, and $\|\boldsymbol{\theta}\|_2$ are bounded by Assumption 1 and $\deg(v)M_{Lvu}$ is continuous. Therefore, if we take $r^{(L)} = O(\frac{1}{\varepsilon'^2} \log \frac{1}{\delta})$ samples, $\Pr[\|\hat{\mathbf{h}}_v^{(L)} - \mathbf{h}_v^{(L)}\|_2 \geq \varepsilon'] \leq \delta$ by the Hoeffding's inequality and equations (2) and (3). Therefore, $\Pr[\|\hat{\mathbf{z}}_v^{(L)} - \mathbf{z}_v^{(L)}\|_2 \geq \varepsilon] \leq \delta$.

Inductive step: It is shown that the statement holds true for $L = l + 1$ if it holds true for $L = l$. The induction hypothesis is $\forall \varepsilon > 0, 1 > \delta > 0, \exists r^{(1)}(\varepsilon, \delta), \dots, r^{(L-1)}(\varepsilon, \delta)$ such that $\forall v \in \mathcal{V}, \Pr[\|\hat{\mathcal{O}}_z^{(L-1)}(v, \varepsilon, \delta) - \mathbf{z}_v\|_2 \geq \varepsilon] \leq \delta$.

Because U_L is uniform continuous,

$$\exists \varepsilon' > 0, \forall \mathbf{z}_v, \mathbf{h}_v, \mathbf{z}'_v, \mathbf{h}'_v, \boldsymbol{\theta}, \|\mathbf{z}_v, \mathbf{h}_v\| - \|\mathbf{z}'_v, \mathbf{h}'_v\|_2 < \varepsilon' \Rightarrow \|U_L(\mathbf{z}_v, \mathbf{h}_v, \boldsymbol{\theta}) - U_L(\mathbf{z}'_v, \mathbf{h}'_v, \boldsymbol{\theta})\|_2 < \varepsilon, \quad (4)$$

where $[\cdot]$ denotes concatenation. By the induction hypothesis,

$$\exists r'^{(1)}, \dots, r'^{(L-1)} \text{ such that } \Pr[\|\hat{\mathcal{O}}_z^{(L-1)}(v) - \mathbf{z}_v^{(L-1)}\|_2 \geq \varepsilon'/\sqrt{2}] \leq \delta/2. \quad (5)$$

holds true. Let

$$\tilde{\mathbf{h}}_v^{(L)} = \frac{\deg(v)}{r^{(L)}} \sum_{u \in \mathcal{S}^{(L)}} M_{Lvu}(\mathbf{z}_v^{(L-1)}, \mathbf{z}_u^{(L-1)}, \mathbf{e}_{vu}, \boldsymbol{\theta}).$$

Let x_k be the k -th sample in $\mathcal{S}^{(L)}$ and $X_k = \deg(v)M_{Lvu}(\mathbf{z}_v^{(L-1)}, \mathbf{z}_{x_k}^{(L-1)}, \mathbf{e}_{vx_k}, \boldsymbol{\theta})$. Then,

$$\mathbb{E}[X_k] = \sum_{u \in \mathcal{N}(v)} M_{Lvu}(\mathbf{z}_v^{(L-1)}, \mathbf{z}_u^{(L-1)}, \mathbf{e}_{vu}, \boldsymbol{\theta}) = \mathbf{h}_v^{(L)}. \quad (6)$$

There exists a constant $C \in \mathbb{R}$ such that for any input satisfying Assumption 1,

$$\|X_k\|_2 < C, \quad (7)$$

because $\|\mathbf{z}_v^{(L-1)}\|_2, \|\mathbf{z}_{x_k}^{(L-1)}\|_2, \|\mathbf{e}_{vx_k}\|_2$, and $\|\boldsymbol{\theta}\|_2$ are bounded by Assumption 1 and Theorem 14, and $\deg(v)M_{Lvu}$ is continuous. If we take $r^{(L)} = O(\frac{1}{\varepsilon'^2} \log \frac{1}{\delta})$, then

$$\Pr[\|\tilde{\mathbf{h}}_v^{(L)} - \mathbf{h}_v^{(L)}\|_2 \geq \varepsilon'/(2\sqrt{2})] \leq \delta/4, \quad (8)$$

by the Hoeffding's inequality and equations (6) and (7). Because $\deg(v)M_{Lvu}$ is uniform continuous,

$$\begin{aligned} \exists \varepsilon'' > 0 \text{ such that } & \|\mathbf{z}_v^{(L-1)}, \mathbf{z}_u^{(L-1)}\| - \|\mathbf{z}'_v{}^{(L-1)}, \mathbf{z}'_u{}^{(L-1)}\|_2 \leq \varepsilon'' \\ \Rightarrow \deg(v) & \|M_{Lvu}(\mathbf{z}_v^{(L-1)}, \mathbf{z}_u^{(L-1)}, \mathbf{e}_{vu}, \boldsymbol{\theta}) - M_{Lvu}(\mathbf{z}'_v{}^{(L-1)}, \mathbf{z}'_u{}^{(L-1)}, \mathbf{e}_{vu}, \boldsymbol{\theta})\|_2 \leq \varepsilon''/(2\sqrt{2}). \end{aligned} \quad (9)$$

By the induction hypothesis,

$$\exists r''^{(1)}, \dots, r''^{(l)} \text{ such that } \Pr[\|\hat{\mathcal{O}}_z^{(L-1)}(v) - \mathbf{z}_v^{(L-1)}\|_2 \geq \varepsilon''/\sqrt{2}] \leq \delta/(8r^{(L)}). \quad (10)$$

Therefore, the probability that the errors of all oracle calls are bounded is

$$\Pr[\exists u \in \mathcal{S}^{(L)}, \|\hat{\mathcal{O}}_z^{(L-1)}(v), \hat{\mathcal{O}}_z^{(L-1)}(u)\| - \|\mathbf{z}_v^{(L-1)}, \mathbf{z}_u^{(L-1)}\|_2 \geq \varepsilon''] \leq \delta/4. \quad (11)$$

By equations (9) and (11),

$$\begin{aligned} & \Pr[\exists u \in \mathcal{S}^{(L)}, \\ & \deg(v) \|M_{Lvu}(\mathbf{z}_v^{(L-1)}, \mathbf{z}_u^{(L-1)}, \mathbf{e}_{vu}, \boldsymbol{\theta}) - M_{Lvu}(\hat{\mathbf{z}}_v^{(L-1)}, \hat{\mathbf{z}}_u^{(L-1)}, \mathbf{e}_{vu}, \boldsymbol{\theta})\|_2 \geq \varepsilon'/(2\sqrt{2})] \leq \delta/4. \end{aligned}$$

$$\Pr[\|\tilde{\mathbf{h}}_v^{(L)} - \hat{\mathbf{h}}_v^{(L)}\|_2 \geq \varepsilon'/(2\sqrt{2})] \leq \delta/4. \quad (12)$$

By the triangular inequality and equations (8) and (12),

$$\Pr[\|\hat{\mathbf{h}}_v^{(L)} - \mathbf{h}_v^{(L)}\|_2 \geq \varepsilon'/\sqrt{2}] \leq \delta/2. \quad (13)$$

Therefore, if we take $r^{(1)} = \max(r'^{(1)}, r''^{(1)})$, \dots , $r^{(L-1)} = \max(r'^{(L-1)}, r''^{(L-1)})$, by equations (5) and (13),

$$\Pr[\|\mathbf{z}_v^{(L-1)}, \mathbf{h}_v^{(L)} - [\hat{\mathcal{O}}_z^{(L-1)}(v), \hat{\mathbf{h}}_v^{(L)}]\|_2 \geq \varepsilon'] \leq \delta. \quad (14)$$

Therefore, by equations (9) and (14),

$$\Pr[\|\hat{\mathbf{z}}_v^{(L)} - \mathbf{z}_v^{(L)}\|_2 \geq \varepsilon] \leq \delta.$$

□

Proof of Theorem 2. We prove this by performing mathematical induction on the number of layers.

Base case: It is shown that the statement holds true for $L = 1$.

If U_L is K -Lipschitz continuous, $\varepsilon' = O(\varepsilon)$ in equation (1). Therefore, $r^{(L)} = O(\frac{1}{\varepsilon^2} \log \frac{1}{\delta})$.

Inductive step: It is shown that the statement holds true for $L = l + 1$ if it holds true for $L = l$.

If U_L and M_{Lvu} are K -Lipschitz continuous, $\varepsilon' = O(\varepsilon)$ in equation (4) and $\varepsilon'' = O(\varepsilon)$ in equation (9). Therefore, $r^{(L)} = O(\frac{1}{\varepsilon^2} \log \frac{1}{\delta})$. We call $\hat{\mathcal{O}}_z^{(L-1)}(v)$ such that $\Pr[\|\hat{\mathcal{O}}_z^{(L-1)}(v) - \mathbf{z}_v^{(L-1)}\|_2 \geq \varepsilon'/\sqrt{2}] \leq \delta/2$ in equation (5). Therefore, $r'^{(1)}, \dots, r'^{(L-1)} = O(\frac{1}{\varepsilon^2} (\log \frac{1}{\varepsilon} + \log \frac{1}{\delta}))$ are sufficient by the induction hypothesis. We call $\hat{\mathcal{O}}_z^{(L-1)}(v)$ such that $\Pr[\|\hat{\mathcal{O}}_z^{(L-1)}(v) - \mathbf{z}_v^{(L-1)}\|_2 \geq \varepsilon''/\sqrt{2}] \leq \delta/(8r^{(L)})$ in equation (10). Therefore, $r''^{(1)}, \dots, r''^{(L-1)} = O(\frac{1}{\varepsilon^2} (\log \frac{1}{\varepsilon} + \log \frac{1}{\delta}))$ are sufficient by the induction hypothesis because $\log \frac{1}{\delta/(8r^{(L)})} = O(\log \frac{1}{\varepsilon} + \log \frac{1}{\delta})$. In total, the complexity is $O(\frac{1}{\varepsilon^2 L} (\log \frac{1}{\varepsilon} + \log \frac{1}{\delta})^{L-1} \log \frac{1}{\delta})$. □

Lemma 15 ((Chazelle et al., 2005)). Let \mathcal{D}^s be Bernoulli($\frac{1+s\varepsilon}{2}$). Let n -dimensional distribution \mathcal{D} be (1) pick $s = 1$ with probability $1/2$ and $s = -1$ otherwise; (2) then draw n values from \mathcal{D}^s . Any probabilistic algorithm that can guess the value of s with a probability error below $1/4$ requires $\Omega(\frac{1}{\varepsilon^2})$ bit lookup on average.

Proof of Theorem 3. We prove there is a counter example in the GraphSAGE-GCN models. Suppose there is an algorithm that approximates the one-layer GraphSAGE-GCN within $o(\varepsilon^2)$ queries. We prove that this algorithm can distinguish \mathcal{D} in Lemma 15 within $o(\varepsilon^2)$ queries and derive a contradiction.

Let σ be any non-constant K -Lipschitz activation function. There exists $a, b \in \mathbb{R}$ ($a > b$) such that $\sigma(a) \neq \sigma(b)$ because σ is not constant. Let $S = \frac{|\sigma(a) - \sigma(b)|}{a - b} > 0$. Let $\varepsilon > 0$ be any sufficiently small positive value and $t \in \{0, 1\}^n$ be a random variable drawn from \mathcal{D} . We prove that we can determine s with high provability within $o(\varepsilon^2)$ queries using the algorithm. Let G be a clique K_n and $\mathbf{W}^{(1)} = 1$. Let us calculate a_ε and b_ε using the following steps: (1) set $a_\varepsilon = a$ and $b_\varepsilon = b$; (2) if $a_\varepsilon - b_\varepsilon < \varepsilon$, return a_ε and b_ε ; (3) $m = \frac{a_\varepsilon + b_\varepsilon}{2}$; (4) if $|\sigma(a_\varepsilon) - \sigma(m)| > |\sigma(m) - \sigma(b_\varepsilon)|$, then set $b_\varepsilon = m$, otherwise $a_\varepsilon = m$; and (5) go back to (2). Here, $\varepsilon/2 \leq a_\varepsilon - b_\varepsilon < \varepsilon$, $a \leq \frac{a_\varepsilon + b_\varepsilon}{2} \leq b$, and $|\sigma(a_\varepsilon) - \sigma(b_\varepsilon)| \geq \frac{S}{2}\varepsilon$ hold true. Let $x_v = \frac{a_\varepsilon + b_\varepsilon}{2} + (2t_v - 1)\frac{a_\varepsilon - b_\varepsilon}{2\varepsilon}$ for all $v \in \mathcal{V}$. Then, $\mathbb{E}[h_v | s = 1] = a_\varepsilon$ and $\mathbb{E}[h_v | s = -1] = b_\varepsilon$. Therefore, $\Pr[|z_v - \sigma(a_\varepsilon)| < \frac{S}{8}\varepsilon | s = 1] \rightarrow 1$ as $n \rightarrow \infty$ and $\Pr[|z_v - \sigma(b_\varepsilon)| < \frac{S}{8}\varepsilon | s = -1] \rightarrow 1$ as $n \rightarrow \infty$ because σ is K -Lipschitz. We set the error tolerance to $\frac{S}{8}\varepsilon$ and n to a sufficiently large number. Then $s = 1$ if $|\hat{z}_v - \sigma(a_\varepsilon)| < \frac{S}{4}\varepsilon$ and $s = -1$ otherwise with high probability. However, the algorithm accesses t (i.e., accesses $\mathcal{O}_{\text{feature}}$) $o(\varepsilon^2)$ times. This contradicts with Lemma 15. □

Lemma 16. Under Assumptions 1, 2 and 3, the norms of the gradients of the message functions and the update functions $\|DU_l(\mathbf{z}_v^{(l-1)}, \mathbf{h}_v^{(l)}, \boldsymbol{\theta})\|_F$, $\|DU_l(\hat{\mathbf{z}}_v^{(l-1)}, \hat{\mathbf{h}}_v^{(l)}, \boldsymbol{\theta})\|_F$, $\|\text{deg}(v)DM_{lvu}(\mathbf{z}_v^{(l-1)}, \mathbf{v}_u^{(l)}, \mathbf{e}_{vu}, \boldsymbol{\theta})\|_F$, and $\|\text{deg}(v)DM_{lvu}(\hat{\mathbf{z}}_v^{(l-1)}, \hat{\mathbf{v}}_u^{(l)}, \mathbf{e}_{vu}, \boldsymbol{\theta})\|_F$ are bounded by a constant $B' \in \mathbb{R}$.

Proof of Lemma 16. The input of each function is bounded by Lemma 14. Because DU_l and $\deg(v)DM_{lvu}$ is uniform continuous, these images are bounded. \square

Proof of Theorem 4. We prove the theorem by performing mathematical induction on the number of layers L .

Base case: It is shown that the statement holds true for $L = 1$.

When the number of layers is one,

$$\begin{aligned} \frac{\partial \mathbf{z}_v^{(L)}}{\partial \boldsymbol{\theta}} &= \frac{\partial U_L}{\partial \boldsymbol{\theta}}(\mathbf{z}_v^{(0)}, \mathbf{h}_v^{(L)}, \boldsymbol{\theta}) + \frac{\partial U_L}{\partial \mathbf{h}_v^{(L)}}(\mathbf{z}_v^{(0)}, \mathbf{h}_v^{(L)}, \boldsymbol{\theta}) \frac{\partial \mathbf{h}_v^{(L)}}{\partial \boldsymbol{\theta}} \\ &= \frac{\partial U_L}{\partial \boldsymbol{\theta}}(\mathbf{z}_v^{(0)}, \mathbf{h}_v^{(L)}, \boldsymbol{\theta}) + \frac{\partial U_L}{\partial \mathbf{h}_v^{(L)}}(\mathbf{z}_v^{(0)}, \mathbf{h}_v^{(L)}, \boldsymbol{\theta}) \sum_{u \in \mathcal{N}(v)} \frac{\partial M_{Lvu}}{\partial \boldsymbol{\theta}}(\mathbf{z}_v^{(0)}, \mathbf{z}_u^{(0)}, \mathbf{e}_{vu}, \boldsymbol{\theta}). \end{aligned}$$

$$\begin{aligned} \frac{\partial \hat{\mathbf{z}}_v^{(L)}}{\partial \boldsymbol{\theta}} &= \frac{\partial U_L}{\partial \boldsymbol{\theta}}(\mathbf{z}_v^{(0)}, \hat{\mathbf{h}}_v^{(L)}, \boldsymbol{\theta}) + \frac{\partial U_L}{\partial \hat{\mathbf{h}}_v^{(L)}}(\mathbf{z}_v^{(0)}, \hat{\mathbf{h}}_v^{(L)}, \boldsymbol{\theta}) \frac{\partial \hat{\mathbf{h}}_v^{(L)}}{\partial \boldsymbol{\theta}} \\ &= \frac{\partial U_L}{\partial \boldsymbol{\theta}}(\mathbf{z}_v^{(0)}, \hat{\mathbf{h}}_v^{(L)}, \boldsymbol{\theta}) + \frac{\partial U_L}{\partial \hat{\mathbf{h}}_v^{(L)}}(\mathbf{z}_v^{(0)}, \hat{\mathbf{h}}_v^{(L)}, \boldsymbol{\theta}) \frac{\deg(v)}{r^{(L)}} \sum_{u \in \mathcal{S}^{(L)}} \frac{\partial M_{Lvu}}{\partial \boldsymbol{\theta}}(\mathbf{z}_v^{(0)}, \mathbf{z}_u^{(0)}, \mathbf{e}_{vu}, \boldsymbol{\theta}). \end{aligned}$$

Because DU_L is uniform continuous,

$$\begin{aligned} &\exists \varepsilon' > 0 \text{ s.t. for all input, } \|\mathbf{h}_v^{(L)} - \hat{\mathbf{h}}_v^{(L)}\|_2 < \varepsilon' \Rightarrow \\ &\left\| \frac{\partial U_L}{\partial \boldsymbol{\theta}}(\mathbf{z}_v^{(0)}, \mathbf{h}_v^{(L)}, \boldsymbol{\theta}) - \frac{\partial U_L}{\partial \boldsymbol{\theta}}(\mathbf{z}_v^{(0)}, \hat{\mathbf{h}}_v^{(L)}, \boldsymbol{\theta}) \right\|_F < \varepsilon/2 \wedge \\ &\left\| \frac{\partial U_L}{\partial \mathbf{h}_v^{(L)}}(\mathbf{z}_v^{(0)}, \mathbf{h}_v^{(L)}, \boldsymbol{\theta}) - \frac{\partial U_L}{\partial \hat{\mathbf{h}}_v^{(L)}}(\mathbf{z}_v^{(0)}, \hat{\mathbf{h}}_v^{(L)}, \boldsymbol{\theta}) \right\|_F < \varepsilon/(4B'). \end{aligned} \quad (15)$$

If we take $r^{(L)} = O(\frac{1}{\varepsilon'^2} \log \frac{1}{\delta})$,

$$\Pr[\|\mathbf{h}_v^{(L)} - \hat{\mathbf{h}}_v^{(L)}\|_2 \geq \varepsilon'] \leq \delta/2 \quad (16)$$

holds true for any input by the argument of the proof of Theorem 1.

Let x_k be the k -th sample in $\mathcal{S}^{(L)}$ and $X_k = \deg(v) \frac{\partial M_{Lvu}}{\partial \boldsymbol{\theta}}(\mathbf{z}_v^{(0)}, \mathbf{z}_u^{(0)}, \mathbf{e}_{vu}, \boldsymbol{\theta})$. Then,

$$\mathbb{E}[X_k] = \sum_{u \in \mathcal{N}(v)} \frac{\partial M_{Lvu}}{\partial \boldsymbol{\theta}}(\mathbf{z}_v^{(0)}, \mathbf{z}_u^{(0)}, \mathbf{e}_{vu}, \boldsymbol{\theta}) = \frac{\partial \mathbf{h}_v^{(L)}}{\partial \boldsymbol{\theta}}. \quad (17)$$

There exists a constant $C \in \mathbb{R}$ such that for any input satisfying Assumption 1,

$$\|X_k\|_2 < C, \quad (18)$$

because $\|\mathbf{z}_v^{(0)}\|_2, \|\mathbf{z}_{x_k}^{(0)}\|_2, \|\mathbf{e}_{vx_k}\|_2$, and $\|\boldsymbol{\theta}\|_2$ are bounded by Assumption 1 and $\deg(v)DM_{Lvu}$ is continuous. Therefore, if we take $r^{(L)} = O(\frac{1}{\varepsilon'^2} \log \frac{1}{\delta})$ samples,

$$\Pr\left[\left\| \frac{\partial \hat{\mathbf{h}}_v^{(L)}}{\partial \boldsymbol{\theta}} - \frac{\partial \mathbf{h}_v^{(L)}}{\partial \boldsymbol{\theta}} \right\|_F \geq \varepsilon/(4B')\right] \leq \delta/2 \quad (19)$$

holds true by the Hoeffding's inequality and equations (17) and (18). If

$$\left\| \frac{\partial \hat{\mathbf{h}}_v^{(L)}}{\partial \boldsymbol{\theta}} - \frac{\partial \mathbf{h}_v^{(L)}}{\partial \boldsymbol{\theta}} \right\|_F < \varepsilon / (4B')$$

and

$$\left\| \frac{\partial U_L}{\partial \mathbf{h}_v^{(L)}}(\mathbf{z}_v^{(0)}, \mathbf{h}_v^{(L)}, \boldsymbol{\theta}) - \frac{\partial U_L}{\partial \hat{\mathbf{h}}_v^{(L)}}(\mathbf{z}_v^{(0)}, \hat{\mathbf{h}}_v^{(L)}, \boldsymbol{\theta}) \right\|_F < \varepsilon / (4B')$$

hold true, then

$$\begin{aligned} & \left\| \frac{\partial \hat{\mathbf{h}}_v^{(L)}}{\partial \boldsymbol{\theta}} \frac{\partial U_L}{\partial \hat{\mathbf{h}}_v^{(L)}}(\mathbf{z}_v^{(0)}, \hat{\mathbf{h}}_v^{(L)}, \boldsymbol{\theta}) - \frac{\partial \mathbf{h}_v^{(L)}}{\partial \boldsymbol{\theta}} \frac{\partial U_L}{\partial \mathbf{h}_v^{(L)}}(\mathbf{z}_v^{(0)}, \mathbf{h}_v^{(L)}, \boldsymbol{\theta}) \right\|_F \\ & \leq \left\| \frac{\partial \hat{\mathbf{h}}_v^{(L)}}{\partial \boldsymbol{\theta}} \frac{\partial U_L}{\partial \hat{\mathbf{h}}_v^{(L)}}(\mathbf{z}_v^{(0)}, \hat{\mathbf{h}}_v^{(L)}, \boldsymbol{\theta}) - \frac{\partial \hat{\mathbf{h}}_v^{(L)}}{\partial \boldsymbol{\theta}} \frac{\partial U_L}{\partial \mathbf{h}_v^{(L)}}(\mathbf{z}_v^{(0)}, \mathbf{h}_v^{(L)}, \boldsymbol{\theta}) \right\|_F \\ & \quad + \left\| \frac{\partial \hat{\mathbf{h}}_v^{(L)}}{\partial \boldsymbol{\theta}} \frac{\partial U_L}{\partial \mathbf{h}_v^{(L)}}(\mathbf{z}_v^{(0)}, \mathbf{h}_v^{(L)}, \boldsymbol{\theta}) - \frac{\partial \mathbf{h}_v^{(L)}}{\partial \boldsymbol{\theta}} \frac{\partial U_L}{\partial \mathbf{h}_v^{(L)}}(\mathbf{z}_v^{(0)}, \mathbf{h}_v^{(L)}, \boldsymbol{\theta}) \right\|_F \\ & = \left\| \frac{\partial \hat{\mathbf{h}}_v^{(L)}}{\partial \boldsymbol{\theta}} \right\|_F \left\| \frac{\partial U_L}{\partial \hat{\mathbf{h}}_v^{(L)}}(\mathbf{z}_v^{(0)}, \hat{\mathbf{h}}_v^{(L)}, \boldsymbol{\theta}) - \frac{\partial U_L}{\partial \mathbf{h}_v^{(L)}}(\mathbf{z}_v^{(0)}, \mathbf{h}_v^{(L)}, \boldsymbol{\theta}) \right\|_F \\ & \quad + \left\| \frac{\partial \hat{\mathbf{h}}_v^{(L)}}{\partial \boldsymbol{\theta}} - \frac{\partial \mathbf{h}_v^{(L)}}{\partial \boldsymbol{\theta}} \right\|_F \left\| \frac{\partial U_L}{\partial \mathbf{h}_v^{(L)}}(\mathbf{z}_v^{(0)}, \mathbf{h}_v^{(L)}, \boldsymbol{\theta}) \right\|_F \\ & \leq B' \left\| \frac{\partial U_L}{\partial \hat{\mathbf{h}}_v^{(L)}}(\mathbf{z}_v^{(0)}, \hat{\mathbf{h}}_v^{(L)}, \boldsymbol{\theta}) - \frac{\partial U_L}{\partial \mathbf{h}_v^{(L)}}(\mathbf{z}_v^{(0)}, \mathbf{h}_v^{(L)}, \boldsymbol{\theta}) \right\|_F + B' \left\| \frac{\partial \hat{\mathbf{h}}_v^{(L)}}{\partial \boldsymbol{\theta}} - \frac{\partial \mathbf{h}_v^{(L)}}{\partial \boldsymbol{\theta}} \right\|_F \\ & < B' \frac{\varepsilon}{4B'} + B' \frac{\varepsilon}{4B'} = \frac{\varepsilon}{2}. \end{aligned}$$

Therefore, $\Pr\left[\left\| \frac{\partial \mathbf{z}_v^{(L)}}{\partial \boldsymbol{\theta}} - \frac{\partial \hat{\mathbf{z}}_v^{(L)}}{\partial \boldsymbol{\theta}} \right\|_F \geq \varepsilon\right] \leq \delta$ by equations (15), (16), and (19).

Inductive step: It is shown that the statement holds true for $L = l + 1$ if it holds true for $L = l$.

$$\begin{aligned} \frac{\partial \mathbf{z}_v^{(L)}}{\partial \boldsymbol{\theta}} &= \frac{\partial U_L}{\partial \boldsymbol{\theta}}(\mathbf{z}_v^{(L-1)}, \mathbf{h}_v^{(L)}, \boldsymbol{\theta}) + \frac{\partial U_L}{\partial \mathbf{z}_v^{(L-1)}}(\mathbf{z}_v^{(L-1)}, \mathbf{h}_v^{(L)}, \boldsymbol{\theta}) \frac{\partial \mathbf{z}_v^{(L-1)}}{\partial \boldsymbol{\theta}} \\ & \quad + \frac{\partial U_L}{\partial \mathbf{h}_v^{(L)}}(\mathbf{z}_v^{(L-1)}, \mathbf{h}_v^{(L)}, \boldsymbol{\theta}) \sum_{u \in \mathcal{N}(v)} \frac{\partial M_{Lvu}}{\partial \boldsymbol{\theta}}(\mathbf{z}_v^{(L-1)}, \mathbf{z}_u^{(L-1)}, \mathbf{e}_{vu}, \boldsymbol{\theta}) \\ & \quad + \frac{\partial U_L}{\partial \mathbf{h}_v^{(L)}}(\mathbf{z}_v^{(L-1)}, \mathbf{h}_v^{(L)}, \boldsymbol{\theta}) \sum_{u \in \mathcal{N}(v)} \frac{\partial M_{Lvu}}{\partial \mathbf{z}_v^{(L-1)}}(\mathbf{z}_v^{(L-1)}, \mathbf{z}_u^{(L-1)}, \mathbf{e}_{vu}, \boldsymbol{\theta}) \frac{\partial \mathbf{z}_v^{(L-1)}}{\partial \boldsymbol{\theta}} \\ & \quad + \frac{\partial U_L}{\partial \mathbf{h}_v^{(L)}}(\mathbf{z}_v^{(L-1)}, \mathbf{h}_v^{(L)}, \boldsymbol{\theta}) \sum_{u \in \mathcal{N}(v)} \frac{\partial M_{Lvu}}{\partial \mathbf{z}_u^{(L-1)}}(\mathbf{z}_v^{(L-1)}, \mathbf{z}_u^{(L-1)}, \mathbf{e}_{vu}, \boldsymbol{\theta}) \frac{\partial \mathbf{z}_u^{(L-1)}}{\partial \boldsymbol{\theta}}. \end{aligned}$$

$$\begin{aligned}
 \frac{\partial \hat{\mathbf{z}}_v^{(L)}}{\partial \boldsymbol{\theta}} &= \frac{\partial U_L}{\partial \boldsymbol{\theta}}(\hat{\mathbf{z}}_v^{(L-1)}, \hat{\mathbf{h}}_v^{(L)}, \boldsymbol{\theta}) + \frac{\partial U_L}{\partial \hat{\mathbf{z}}_v^{(L-1)}}(\hat{\mathbf{z}}_v^{(L-1)}, \hat{\mathbf{h}}_v^{(L)}, \boldsymbol{\theta}) \frac{\partial \hat{\mathbf{z}}_v^{(L-1)}}{\partial \boldsymbol{\theta}} \\
 &+ \frac{\partial U_L}{\partial \hat{\mathbf{h}}_v^{(L)}}(\hat{\mathbf{z}}_v^{(L-1)}, \hat{\mathbf{h}}_v^{(L)}, \boldsymbol{\theta}) \frac{\deg(v)}{r^{(L)}} \sum_{u \in \mathcal{S}^{(L)}} \frac{\partial M_{Lvu}}{\partial \boldsymbol{\theta}}(\hat{\mathbf{z}}_v^{(L-1)}, \hat{\mathbf{z}}_u^{(L-1)}, \mathbf{e}_{vu}, \boldsymbol{\theta}) \\
 &+ \frac{\partial U_L}{\partial \hat{\mathbf{h}}_v^{(L)}}(\hat{\mathbf{z}}_v^{(L-1)}, \hat{\mathbf{h}}_v^{(L)}, \boldsymbol{\theta}) \frac{\deg(v)}{r^{(L)}} \sum_{u \in \mathcal{S}^{(L)}} \frac{\partial M_{Lvu}}{\partial \hat{\mathbf{z}}_v^{(L-1)}}(\hat{\mathbf{z}}_v^{(L-1)}, \hat{\mathbf{z}}_u^{(L-1)}, \mathbf{e}_{vu}, \boldsymbol{\theta}) \frac{\partial \hat{\mathbf{z}}_v^{(L-1)}}{\partial \boldsymbol{\theta}} \\
 &+ \frac{\partial U_L}{\partial \hat{\mathbf{h}}_v^{(L)}}(\hat{\mathbf{z}}_v^{(L-1)}, \hat{\mathbf{h}}_v^{(L)}, \boldsymbol{\theta}) \frac{\deg(v)}{r^{(L)}} \sum_{u \in \mathcal{S}^{(L)}} \frac{\partial M_{Lvu}}{\partial \hat{\mathbf{z}}_u^{(L-1)}}(\hat{\mathbf{z}}_v^{(L-1)}, \hat{\mathbf{z}}_u^{(L-1)}, \mathbf{e}_{vu}, \boldsymbol{\theta}) \frac{\partial \hat{\mathbf{z}}_u^{(L-1)}}{\partial \boldsymbol{\theta}}.
 \end{aligned}$$

Because DU_L is uniform continuous,

$$\begin{aligned}
 \exists \varepsilon' > 0 \text{ s.t. for all input, } &\|[\mathbf{z}_v^{(L-1)}, \mathbf{h}_v^{(L)}] - [\hat{\mathbf{z}}_v^{(L-1)}, \hat{\mathbf{h}}_v^{(L)}]\|_2 < \varepsilon' \Rightarrow \\
 &\left\| \frac{\partial U_L}{\partial \boldsymbol{\theta}}(\mathbf{z}_v^{(L-1)}, \mathbf{h}_v^{(L)}, \boldsymbol{\theta}) - \frac{\partial U_L}{\partial \boldsymbol{\theta}}(\hat{\mathbf{z}}_v^{(L-1)}, \hat{\mathbf{h}}_v^{(L)}, \boldsymbol{\theta}) \right\|_F < O(\varepsilon) \wedge \\
 &\left\| \frac{\partial U_L}{\partial \hat{\mathbf{h}}_v^{(L)}}(\mathbf{z}_v^{(L-1)}, \mathbf{h}_v^{(L)}, \boldsymbol{\theta}) - \frac{\partial U_L}{\partial \hat{\mathbf{h}}_v^{(L)}}(\hat{\mathbf{z}}_v^{(L-1)}, \hat{\mathbf{h}}_v^{(L)}, \boldsymbol{\theta}) \right\|_F < O(\varepsilon) \wedge \\
 &\left\| \frac{\partial U_L}{\partial \mathbf{z}_v^{(L-1)}}(\mathbf{z}_v^{(L-1)}, \mathbf{h}_v^{(L)}, \boldsymbol{\theta}) - \frac{\partial U_L}{\partial \hat{\mathbf{z}}_v^{(L-1)}}(\hat{\mathbf{z}}_v^{(L-1)}, \hat{\mathbf{h}}_v^{(L)}, \boldsymbol{\theta}) \right\|_F < O(\varepsilon). \tag{20}
 \end{aligned}$$

Because $\deg(v)DM_{Lvu}$ is uniform continuous,

$$\begin{aligned}
 \exists \varepsilon'' > 0 \text{ s.t. for all input, } &\|[\mathbf{z}_v^{(L-1)}, \mathbf{z}_u^{(L-1)}] - [\hat{\mathbf{z}}_v^{(L-1)}, \hat{\mathbf{z}}_u^{(L-1)}]\|_2 < \varepsilon'' \Rightarrow \\
 (\deg(v) \left\| \frac{\partial M_{Lvu}}{\partial \boldsymbol{\theta}}(\mathbf{z}_v^{(L-1)}, \mathbf{z}_u^{(L-1)}, \mathbf{e}_{vu}, \boldsymbol{\theta}) - \frac{\partial M_{Lvu}}{\partial \boldsymbol{\theta}}(\hat{\mathbf{z}}_v^{(L-1)}, \hat{\mathbf{z}}_u^{(L-1)}, \mathbf{e}_{vu}, \boldsymbol{\theta}) \right\|_F < O(\varepsilon) \wedge \\
 \deg(v) \left\| \frac{\partial M_{Lvu}}{\partial \hat{\mathbf{h}}_v^{(L)}}(\mathbf{z}_v^{(L-1)}, \mathbf{z}_u^{(L-1)}, \mathbf{e}_{vu}, \boldsymbol{\theta}) - \frac{\partial M_{Lvu}}{\partial \hat{\mathbf{h}}_v^{(L)}}(\hat{\mathbf{z}}_v^{(L-1)}, \hat{\mathbf{z}}_u^{(L-1)}, \mathbf{e}_{vu}, \boldsymbol{\theta}) \right\|_F < O(\varepsilon) \wedge \\
 \deg(v) \left\| \frac{\partial M_{Lvu}}{\partial \mathbf{z}_v^{(L-1)}}(\mathbf{z}_v^{(L-1)}, \mathbf{z}_u^{(L-1)}, \mathbf{e}_{vu}, \boldsymbol{\theta}) - \frac{\partial M_{Lvu}}{\partial \hat{\mathbf{z}}_v^{(L-1)}}(\hat{\mathbf{z}}_v^{(L-1)}, \hat{\mathbf{z}}_u^{(L-1)}, \mathbf{e}_{vu}, \boldsymbol{\theta}) \right\|_F < O(\varepsilon)). \tag{21}
 \end{aligned}$$

By the argument of the proof of Theorem 1, if we take sufficiently large number of samples,

$$\Pr[\|\mathbf{z}_v^{(L-1)} - \hat{\mathbf{z}}_v^{(L-1)}\|_2 \geq O(\min(\varepsilon', \varepsilon''))] \leq O(\varepsilon\delta), \tag{22}$$

$$\Pr[\|\mathbf{h}_v^{(L)} - \hat{\mathbf{h}}_v^{(L)}\|_2 \geq O(\varepsilon')] \leq O(\delta). \tag{23}$$

By the induction hypothesis, there exists $r^{(1)}, \dots, r^{(L-1)}$ such that

$$\Pr\left[\left\| \frac{\partial \mathbf{z}_u^{(L-1)}}{\partial \boldsymbol{\theta}} - \frac{\partial \hat{\mathbf{z}}_u^{(L-1)}}{\partial \boldsymbol{\theta}} \right\|_F \geq O(\varepsilon)\right] \leq O(\varepsilon\delta),$$

$$\Pr\left[\left\| \frac{\partial \mathbf{z}_v^{(L-1)}}{\partial \boldsymbol{\theta}} - \frac{\partial \hat{\mathbf{z}}_v^{(L-1)}}{\partial \boldsymbol{\theta}} \right\|_F \geq O(\varepsilon)\right] \leq O(\varepsilon\delta),$$

If we take $r^{(L)} = O(\frac{1}{\varepsilon^2} \log \frac{1}{\delta})$,

$$\Pr\left[\left\| \sum_{u \in \mathcal{N}(v)} \frac{\partial M_{Lvu}}{\partial \boldsymbol{\theta}}(\mathbf{z}_v^{(L-1)}, \mathbf{z}_u^{(L-1)}, \mathbf{e}_{vu}, \boldsymbol{\theta}) - \frac{\deg(v)}{r^{(L)}} \sum_{u \in \mathcal{S}^{(L)}} \frac{\partial M_{Lvu}}{\partial \boldsymbol{\theta}}(\mathbf{z}_v^{(L-1)}, \mathbf{z}_u^{(L-1)}, \mathbf{e}_{vu}, \boldsymbol{\theta}) \right\| \geq O(\varepsilon) \right] \leq O(\delta), \quad (24)$$

$$\Pr\left[\left\| \sum_{u \in \mathcal{N}(v)} \frac{\partial M_{Lvu}}{\partial \mathbf{z}_v^{(L-1)}}(\mathbf{z}_v^{(L-1)}, \mathbf{z}_u^{(L-1)}, \mathbf{e}_{vu}, \boldsymbol{\theta}) \frac{\partial \mathbf{z}_v^{(L-1)}}{\partial \boldsymbol{\theta}} - \frac{\deg(v)}{r^{(L)}} \sum_{u \in \mathcal{S}^{(L)}} \frac{\partial M_{Lvu}}{\partial \mathbf{z}_v^{(L-1)}}(\mathbf{z}_v^{(L-1)}, \mathbf{z}_u^{(L-1)}, \mathbf{e}_{vu}, \boldsymbol{\theta}) \frac{\partial \mathbf{z}_v^{(L-1)}}{\partial \boldsymbol{\theta}} \right\| \geq O(\varepsilon) \right] \leq O(\delta), \quad (25)$$

$$\Pr\left[\left\| \sum_{u \in \mathcal{N}(v)} \frac{\partial M_{Lvu}}{\partial \mathbf{z}_u^{(L-1)}}(\mathbf{z}_v^{(L-1)}, \mathbf{z}_u^{(L-1)}, \mathbf{e}_{vu}, \boldsymbol{\theta}) \frac{\partial \mathbf{z}_u^{(L-1)}}{\partial \boldsymbol{\theta}} - \frac{\deg(v)}{r^{(L)}} \sum_{u \in \mathcal{S}^{(L)}} \frac{\partial M_{Lvu}}{\partial \mathbf{z}_u^{(L-1)}}(\mathbf{z}_v^{(L-1)}, \mathbf{z}_u^{(L-1)}, \mathbf{e}_{vu}, \boldsymbol{\theta}) \frac{\partial \mathbf{z}_u^{(L-1)}}{\partial \boldsymbol{\theta}} \right\| \geq O(\varepsilon) \right] \leq O(\delta), \quad (26)$$

holds true by the Hoeffding's inequality. Therefore,

$$\Pr\left[\left\| \sum_{u \in \mathcal{N}(v)} \frac{\partial M_{Lvu}}{\partial \boldsymbol{\theta}}(\mathbf{z}_v^{(L-1)}, \mathbf{z}_u^{(L-1)}, \mathbf{e}_{vu}, \boldsymbol{\theta}) - \frac{\deg(v)}{r^{(L)}} \sum_{u \in \mathcal{S}^{(L)}} \frac{\partial M_{Lvu}}{\partial \boldsymbol{\theta}}(\hat{\mathbf{z}}_v^{(L-1)}, \hat{\mathbf{z}}_u^{(L-1)}, \mathbf{e}_{vu}, \boldsymbol{\theta}) \right\| \geq O(\varepsilon) \right] \leq O(\delta), \quad (27)$$

$$\Pr\left[\left\| \sum_{u \in \mathcal{N}(v)} \frac{\partial M_{Lvu}}{\partial \mathbf{z}_v^{(L-1)}}(\mathbf{z}_v^{(L-1)}, \mathbf{z}_u^{(L-1)}, \mathbf{e}_{vu}, \boldsymbol{\theta}) \frac{\partial \mathbf{z}_v^{(L-1)}}{\partial \boldsymbol{\theta}} - \frac{\deg(v)}{r^{(L)}} \sum_{u \in \mathcal{S}^{(L)}} \frac{\partial M_{Lvu}}{\partial \hat{\mathbf{z}}_v^{(L-1)}}(\hat{\mathbf{z}}_v^{(L-1)}, \hat{\mathbf{z}}_u^{(L-1)}, \mathbf{e}_{vu}, \boldsymbol{\theta}) \frac{\partial \hat{\mathbf{z}}_v^{(L-1)}}{\partial \boldsymbol{\theta}} \right\| \geq O(\varepsilon) \right] \leq O(\delta), \quad (28)$$

$$\Pr\left[\left\| \sum_{u \in \mathcal{N}(v)} \frac{\partial M_{Lvu}}{\partial \mathbf{z}_u^{(L-1)}}(\mathbf{z}_v^{(L-1)}, \mathbf{z}_u^{(L-1)}, \mathbf{e}_{vu}, \boldsymbol{\theta}) \frac{\partial \mathbf{z}_u^{(L-1)}}{\partial \boldsymbol{\theta}} - \frac{\deg(v)}{r^{(L)}} \sum_{u \in \mathcal{S}^{(L)}} \frac{\partial M_{Lvu}}{\partial \hat{\mathbf{z}}_u^{(L-1)}}(\hat{\mathbf{z}}_v^{(L-1)}, \hat{\mathbf{z}}_u^{(L-1)}, \mathbf{e}_{vu}, \boldsymbol{\theta}) \frac{\partial \hat{\mathbf{z}}_u^{(L-1)}}{\partial \boldsymbol{\theta}} \right\| \geq O(\varepsilon) \right] \leq O(\delta), \quad (29)$$

holds true by equations (20), (21), (22), (23), (24), (25), and (26).

Therefore, if we take $r^{(1)}, \dots, r^{(L)}$ sufficiently large, $\Pr\left[\left\| \frac{\partial \mathbf{z}_v^{(L)}}{\partial \boldsymbol{\theta}} - \frac{\partial \hat{\mathbf{z}}_v^{(L)}}{\partial \boldsymbol{\theta}} \right\|_F \geq \varepsilon \right] \leq \delta$ holds true by equations (20), (21), (22), (23), (27), (28), and (29).

□

Proof of Theorem 5. We prove this by performing mathematical induction on the number of layers.

Base case: It is shown that the statement holds true for $L = 1$.

If DU_L is K' -Lipschitz continuous, $\varepsilon' = O(\varepsilon)$ in equation (15). Therefore, $r^{(L)} = O(\frac{1}{\varepsilon^2} \log \frac{1}{\delta})$ is sufficient.

Inductive step: It is shown that the statement holds true for $L = l + 1$ if it holds true for $L = l$.

If DU_L and $\deg(v)DU_{Lvu}$ is K' -Lipschitz continuous, $\varepsilon' = O(\varepsilon)$ in equation (20) and $\varepsilon'' = O(\varepsilon)$ in equation (21). Therefore, $r^{(L)} = O(\frac{1}{\varepsilon^2} \log \frac{1}{\delta})$ and $r^{(1)}, \dots, r^{(L-1)} = O(\frac{1}{\varepsilon^2} (\log \frac{1}{\varepsilon} + \log \frac{1}{\delta}))$ are sufficient. \square

Proof of Proposition 6. We show that one-layer GraphSAGE-GCN whose activation function is not constant cannot be approximated in constant time if $\|x_v\|_2$ or $\|\theta\|_2$ are not bounded. There exists $a \in \mathbb{R}$ such that $\sigma(a) \neq \sigma(0)$ because σ is not constant. We consider the following two types of inputs:

- G is the clique K_n , $\mathbf{W}^{(1)} = \mathbf{I}$, and $\mathbf{x}_i = 0$ for all nodes $i \in \mathcal{V}$.
- G is the clique K_n , $\mathbf{W}^{(1)} = \mathbf{I}$, $\mathbf{x}_i = 0 (i \neq v)$ for some $v \in \mathcal{V}$, and $\mathbf{x}_v = an$.

Then, for the former input, $z_v^{(1)} = \sigma(0)$. For the latter type of inputs, $z_v^{(1)} = \sigma(a)$. Let \mathcal{A} be an arbitrary constant algorithm and C be the number of queries \mathcal{A} makes when we set $\varepsilon = |\sigma(a) - \sigma(0)|/3$. When \mathcal{A} calculates the embedding of $u \neq v \in \mathcal{V}$, the states of all nodes but u are symmetrical until \mathcal{A} makes a query about that node. Therefore, if n is sufficiently large, \mathcal{A} does not make any query about v with high probability (i.e., at least $(1 - \frac{1}{n-1})^C$). If \mathcal{A} does not make any query about v , the state of \mathcal{A} is the same for both types of inputs. If the approximation error is less than ε for the first type of inputs, the approximation error is larger than ε for the second type of inputs by the triangle inequality and vice versa. Therefore, \mathcal{A} fails to approximate the embeddings of either type of inputs with the absolute error of at most ε . As for θ , we set $\mathbf{W}^{(1)} = an$ and $\mathbf{x}_v = 1$ for the second type of inputs. Then, the same argument follows. \square

Proof of Proposition 7. We consider the one-layer GraphSAGE-GCN with ReLU and normalization (i.e., $\sigma(\mathbf{x}) = \text{RELU}(\mathbf{x})/\|\text{RELU}(\mathbf{x})\|_2$). We use the following two types of inputs:

- G is the clique K_n , $\mathbf{W}^{(1)}$ is the identity matrix \mathbf{I}_2 , $\mathbf{x}_i = (0, 0)^\top (i \neq v)$ for some node $v \in \mathcal{V}$, and $\mathbf{x}_v = (1, 0)^\top$.
- G is the clique K_n , $\mathbf{W}^{(1)}$ is the identity matrix \mathbf{I}_2 , $\mathbf{x}_i = (0, 0)^\top (i \neq v)$ for some node $v \in \mathcal{V}$, and $\mathbf{x}_v = (0, 1)^\top$.

Then, for the former type of inputs, $\mathbf{h}_i = (1/n, 0)^\top$, $\mathbf{z}_i = (1, 0)^\top$, and $\frac{\partial z_{i2}}{\partial W_{21}} = 1$ for all $i \in \mathcal{V}$. For the latter type of inputs, $\mathbf{h}_i = (0, 1/n)^\top$, $\mathbf{z}_i = (0, 1)^\top$, and $\frac{\partial z_{i2}}{\partial W_{21}} = 0$ for all $i \in \mathcal{V}$. Let \mathcal{A} be an arbitrary constant algorithm and C be the number of queries \mathcal{A} makes when we set $\varepsilon = 1/3$. When \mathcal{A} calculates the embedding or gradient of $u \neq v \in \mathcal{V}$, the states of all nodes but u are symmetrical until \mathcal{A} makes a query about that node. Therefore, if n is sufficiently large, \mathcal{A} does not make any query about v with high probability (i.e., at least $(1 - \frac{1}{n-1})^C$). If \mathcal{A} does not make any query about v , the state of \mathcal{A} is the same for both types of inputs. If the approximation error is less than ε for the first type of inputs, the approximation error is larger than ε for the second type of inputs by the triangle inequality and vice versa. Therefore, \mathcal{A} fails to approximate the embeddings and gradients of either type of inputs with the absolute error of at most ε . \square

Proof of Proposition 8. We consider the one-layer GraphSAGE-GCN with ReLU (i.e., $\sigma(\mathbf{x}) = \text{RELU}(\mathbf{x})$). We use the following two types of inputs:

- G is the clique K_n , $\mathbf{W}^{(1)} = (-1, 1)$, $\mathbf{x}_i = (1, 1)^\top (i \neq v)$ for some node $v \in \mathcal{V}$, and $\mathbf{x}_v = (1, 2)^\top$.
- G is the clique K_n , $\mathbf{W}^{(1)} = (-1, 1)$, $\mathbf{x}_i = (1, 1)^\top (i \neq v)$ for some node $v \in \mathcal{V}$, and $\mathbf{x}_v = (1, 0)^\top$.

Then, for the former type of inputs, $\text{MEAN}(\{\mathbf{x}_u \mid u \in \mathcal{N}(v)\}) = (1, 1 + \frac{1}{n})^\top$, $\mathbf{h}_v = \mathbf{z}_v = \frac{1}{n}$, and $\frac{\partial z_v}{\partial \mathbf{W}} = (1, 1 + \frac{1}{n})$ for all $i \in \mathcal{V}$. For the latter type of inputs, $\text{MEAN}(\{\mathbf{x}_u \mid u \in \mathcal{N}(v)\}) = (1, 1 - \frac{1}{n})^\top$, $\mathbf{h}_v = -\frac{1}{n}$, $\mathbf{z}_v = 0$, and $\frac{\partial z_v}{\partial \mathbf{W}} = (0, 0)$ for all $i \in \mathcal{V}$. Let \mathcal{A} be an arbitrary constant algorithm and C be the number of queries \mathcal{A} makes when we set $\varepsilon = 1/3$. When \mathcal{A} calculates the gradient of $u \neq v \in \mathcal{V}$, the states of all nodes but u are symmetrical until \mathcal{A} makes a query about that node.

Therefore, if n is sufficiently large, \mathcal{A} does not make any query about v with high probability (i.e., at least $(1 - \frac{1}{n-1})^C$). If \mathcal{A} does not make any query about v , the state of \mathcal{A} is the same for both types of inputs. If the approximation error is less than ε for the first type of inputs, the approximation error is larger than ε for the second type of inputs by the triangle inequality and vice versa. Therefore, \mathcal{A} fails to approximate the gradients of either type of inputs with the absolute error of at most ε . \square

Proof of Proposition 9. We consider the one-layer GraphSAGE-pool whose activation function satisfies $\sigma(1) \neq \sigma(0)$ and the following two types of inputs:

- G is the clique K_n , $\mathbf{W}^{(1)} = 1$, $\mathbf{b} = 0$, and $\mathbf{x}_i = 0$ for all nodes $v \in \mathcal{V}$.
- G is the clique K_n , $\mathbf{W}^{(1)} = 1$, $\mathbf{b} = 0$, $\mathbf{x}_i = 0$ ($i \neq v$) for some node $v \in \mathcal{V}$, and $\mathbf{x}_v = 1$.

Then, for the former type of inputs, $\mathbf{z}_i = \sigma(0)$ for all $i \in \mathcal{V}$. For the latter type of inputs, $\mathbf{z}_i = \sigma(1)$ for all $i \in \mathcal{V}$. Let \mathcal{A} be an arbitrary constant algorithm and C be the number of queries \mathcal{A} makes when we set $\varepsilon = |\sigma(1) - \sigma(0)|/3$. When \mathcal{A} calculates the embedding of $u \neq v \in \mathcal{V}$, the states of all nodes but u are symmetrical until \mathcal{A} makes a query about that node. Therefore, if n is sufficiently large, \mathcal{A} does not make any query about v with high probability (i.e., at least $(1 - \frac{1}{n-1})^C$). If \mathcal{A} does not make any query about v , the state of \mathcal{A} is the same for both types of inputs. If the approximation error is less than ε for the first type of inputs, the approximation error is larger than ε for the second type of inputs by the triangle inequality and vice versa. Therefore, \mathcal{A} fails to approximate the embeddings of either type of inputs with the absolute error of at most ε . \square

Proof of Proposition 10. We consider the one-layer GCNs whose activation function satisfies $\sigma(1) \neq \sigma(0)$. We use the following two types of inputs:

- G is a star graph, where $v \in \mathcal{V}$ is the center of G , $\mathbf{W}^{(1)} = 1$, and all features are 0.
- G is a star graph, where $v \in \mathcal{V}$ is the center of G , $\mathbf{W}^{(1)} = 1$, and the features of $\sqrt{2n}$ leafs are 1 and the features of other nodes are 0.

Then, for the former type of inputs, $\mathbf{z}_v = \sigma(0)$. For the latter type of inputs, $\mathbf{z}_v = \sigma(1)$. Let \mathcal{A} be an arbitrary constant algorithm and C be the number of queries \mathcal{A} makes when we set $\varepsilon = |\sigma(1) - \sigma(0)|/3$. When \mathcal{A} calculates the embedding of $u \in \mathcal{V}$ that $\mathbf{x}_u = 0$, the states of all nodes but u are symmetrical until \mathcal{A} makes a query about that node. Therefore, if n is sufficiently large, \mathcal{A} does not make any query about v with high probability (i.e., at least $(1 - \frac{\sqrt{2n}}{n-1})^C$). If \mathcal{A} does not make any query about v , the state of \mathcal{A} is the same for both types of inputs. If the approximation error is less than ε for the first type of inputs, the approximation error is larger than ε for the second type of inputs by the triangle inequality and vice versa. Therefore, \mathcal{A} fails to approximate the embeddings of either type of inputs with the absolute error of at most ε . \square

We prove the following lemma to prove Proposition 11.

Lemma 17. *If Assumptions 1 holds true and σ is Lipschitz continuous, $\|\mathbf{z}_v^{(l)}\|_2$ and $\|\hat{\mathbf{z}}_v^{(l)}\|_2$ ($l = 1, \dots, L$) of the GAT model are bounded by a constant*

Proof of Lemma 17. We prove this by performing mathematical induction on the number of layers. The norm of the input of the first layer is bounded by Assumption 1. If $\|\mathbf{z}_u^{(l-1)}\|_2$ and $\|\hat{\mathbf{z}}_u^{(l-1)}\|_2$ are bounded for all $u \in \mathcal{V}$, $\|\mathbf{h}_v^{(l)}\|_2$ and $\|\hat{\mathbf{h}}_v^{(l)}\|_2$ are bounded because $\mathbf{h}_v^{(l)}$ and $\hat{\mathbf{h}}_v^{(l)}$ are the weighted sum of $\mathbf{z}_u^{(l-1)}$ and $\hat{\mathbf{z}}_u^{(l-1)}$. Therefore, $\|\mathbf{z}_u^{(l)}\|_2$ and $\|\hat{\mathbf{z}}_u^{(l)}\|_2$ are bounded because U_l is continuous. \square

Proof of Proposition 11. We prove the theorem by performing mathematical induction on the number of layers L .

Base case: It is shown that the statement holds true for $L = 1$.

Because U_L is Lipschitz continuous,

$$\forall \mathbf{z}_v, \mathbf{h}_v, \mathbf{h}'_v, \boldsymbol{\theta}, \|\mathbf{h}_v - \mathbf{h}'_v\|_2 < O(\varepsilon) \Rightarrow \|U_L(\mathbf{z}_v, \mathbf{h}_v, \boldsymbol{\theta}) - U_L(\mathbf{z}_v, \mathbf{h}'_v, \boldsymbol{\theta})\|_2 < \varepsilon. \quad (30)$$

Let $e_u = \exp(\text{LEAKYRELU}(\mathbf{a}^{(l)\top} [\mathbf{W}^{(0)} \mathbf{z}_v^{(0)}, \mathbf{W}^{(0)} \mathbf{z}_u^{(0)} u]))$. Then,

$$\begin{aligned} & \hat{\mathbf{h}}_v^{(L)} - \mathbf{h}_v^{(L)} \\ &= \sum_{u \in \mathcal{S}^{(L)}} \hat{\alpha}_{vu} \mathbf{z}_u^{(0)} - \sum_{u \in \mathcal{N}(v)} \alpha_{vu} \mathbf{z}_u^{(0)} \\ &= \frac{1}{r^{(L)}} \sum_{u \in \mathcal{S}^{(L)}} \frac{e_u}{\frac{1}{r^{(L)}} \sum_{u' \in \mathcal{S}^{(L)}} e_{u'}} \mathbf{z}_u^{(0)} - \frac{1}{\text{deg}(v)} \sum_{u \in \mathcal{N}(v)} \frac{e_u}{\frac{1}{\text{deg}(v)} \sum_{u' \in \mathcal{N}(v)} e_{u'}} \mathbf{z}_u^{(0)}. \end{aligned}$$

Let x_k be the k -th sample in $\mathcal{S}^{(L)}$ and $X_k = e_{x_k}$. Then,

$$\mathbb{E}[X_k] = \frac{1}{\mathcal{N}(v)} \sum_{u \in \mathcal{N}(v)} e_u. \quad (31)$$

There exists a constant $c > 0, C > 0$ such that for any input satisfying Assumption 1,

$$c < |X_k| < C, \quad (32)$$

because $\|\mathbf{z}_v^{(0)}\|_2, \|\mathbf{z}_{x_k}^{(0)}\|_2, \|\mathbf{W}^{(0)}\|_F$, and $\|\mathbf{a}^{(0)}\|_2$ are bounded by Assumption 1. Therefore, if we take $r^{(L)} = O(\frac{1}{\varepsilon^2} \log \frac{1}{\delta})$ samples,

$$\Pr\left[\left|\frac{1}{r^{(L)}} \sum_{u \in \mathcal{S}^{(L)}} e_u - \frac{1}{\mathcal{N}(v)} \sum_{u \in \mathcal{N}(v)} e_u\right| \geq O(\varepsilon)\right] \leq O(\delta)$$

by the Hoeffding's inequality and equations (31) and (32). Because $f(x) = 1/x$ is Lipschitz continuous in $x > c > 0$,

$$\Pr\left[\left|\frac{1}{\frac{1}{r^{(L)}} \sum_{u \in \mathcal{S}^{(L)}} e_u} - \frac{1}{\frac{1}{\mathcal{N}(v)} \sum_{u \in \mathcal{N}(v)} e_u}\right| \geq O(\varepsilon)\right] \leq O(\delta) \quad (33)$$

Let

$$Y_k = \frac{e_{x_k}}{\frac{1}{\mathcal{N}(v)} \sum_{u' \in \mathcal{N}(v)} e_{u'}} \mathbf{z}_{x_k}^{(0)}.$$

Then,

$$\mathbb{E}[Y_k] = \frac{1}{\mathcal{N}(v)} \sum_{u \in \mathcal{N}(v)} \frac{e_u}{\frac{1}{\mathcal{N}(v)} \sum_{u' \in \mathcal{N}(v)} e_{u'}} \mathbf{z}_u^{(0)}. \quad (34)$$

There exists a constant $C' \in \mathbb{R}$ such that for any input satisfying Assumption 1,

$$\|Y_k\|_2 < C' \quad (35)$$

holds true because $\|\mathbf{z}_u^{(0)}\|_2$ are bounded, and $c < |e_u| < C$. Therefore, if we take $r^{(L)} = O(\frac{1}{\varepsilon^2} \log \frac{1}{\delta})$ samples,

$$\begin{aligned} & \Pr\left[\left\|\frac{1}{r^{(L)}} \sum_{u \in \mathcal{S}^{(L)}} \frac{e_u}{\frac{1}{\text{deg}(v)} \sum_{u' \in \mathcal{N}(v)} e_{u'}} \mathbf{z}_u^{(0)}\right.\right. \\ & \quad \left.\left. - \frac{1}{\text{deg}(v)} \sum_{u \in \mathcal{N}(v)} \frac{e_u}{\frac{1}{\text{deg}(v)} \sum_{u' \in \mathcal{N}(v)} e_{u'}} \mathbf{z}_u^{(0)}\right\|_2 \geq O(\varepsilon)\right] \leq O(\delta) \end{aligned} \quad (36)$$

holds true by the Hoeffding's inequality and equations (34) and (35). Therefore,

$$\Pr\left[\left\|\frac{1}{r^{(L)}} \sum_{u \in \mathcal{S}^{(L)}} \frac{e_u}{\frac{1}{r^{(L)}} \sum_{u' \in \mathcal{S}^{(L)}} e_{u'}} \mathbf{z}_u^{(0)} - \frac{1}{\deg(v)} \sum_{u \in \mathcal{N}(v)} \frac{e_u}{\frac{1}{\deg(v)} \sum_{u' \in \mathcal{N}(v)} e_{u'}} \mathbf{z}_u^{(0)}\right\|_2 \geq O(\varepsilon)\right] \leq O(\delta) \quad (37)$$

holds true by the triangle inequality and equations (33) and (36), and $\Pr[\|\hat{\mathbf{z}}_v^{(L)} - \mathbf{z}_v^{(L)}\|_2 \geq \varepsilon] \leq \delta$ holds true by equations (30) and (37).

Inductive step: It is shown that the statement holds true for $L = l + 1$ if it holds true for $L = l$.

Because U_L is Lipschitz continuous,

$$\forall \mathbf{z}_v, \mathbf{h}_v, \mathbf{h}'_v, \boldsymbol{\theta}, \|\mathbf{h}_v - \mathbf{h}'_v\|_2 < O(\varepsilon) \Rightarrow \|U_L(\mathbf{z}_v, \mathbf{h}_v, \boldsymbol{\theta}) - U_L(\mathbf{z}_v, \mathbf{h}'_v, \boldsymbol{\theta})\|_2 < \varepsilon \quad (38)$$

holds true.

$$\Pr\left[\left\|\frac{1}{r^{(L)}} \sum_{u \in \mathcal{S}^{(L)}} \frac{e_u}{\frac{1}{r^{(L)}} \sum_{u' \in \mathcal{S}^{(L)}} e_{u'}} \mathbf{z}_u^{(L-1)} - \frac{1}{\deg(v)} \sum_{u \in \mathcal{N}(v)} \frac{e_u}{\frac{1}{\deg(v)} \sum_{u' \in \mathcal{N}(v)} e_{u'}} \mathbf{z}_u^{(L-1)}\right\|_2 \geq O(\varepsilon)\right] \leq O(\delta) \quad (39)$$

holds true by the same argument as the base step. If we take $r^{(1)}, \dots, r^{(L-1)} = O(\frac{1}{\varepsilon^2}(\log \frac{1}{\varepsilon} + \log \frac{1}{\delta}))$ samples,

$$\Pr[\|\hat{\mathbf{z}}_u^{(L-1)} - \mathbf{z}_u^{(L-1)}\|_2 \geq O(\varepsilon)] \leq O(\varepsilon\delta) \quad (40)$$

holds true by the induction hypothesis. Therefore, $\Pr[\|\hat{\mathbf{z}}_v^{(L)} - \mathbf{z}_v^{(L)}\|_2 \geq \varepsilon] \leq \delta$ holds true by equations (38), (39), and (40). □

D. Computational Model Assumptions

In this study, we modeled our algorithm as an oracle machine that can make queries about the input and measured the complexity by query complexity. Modeling our algorithm as an oracle machine and measuring the complexity by query complexity are reasonable owing to the following reasons:

- In a realistic setting, data is stored in a storage or cloud and we may not be able to load all the information of a huge network on to the main memory. Sometimes the input graph is constructed on demand (e.g., in web graph mining, the edge information is retrieved when queried). In such cases, reducing the number of queries is crucial because accessing storage or cloud is very expensive.
- Our algorithm executes a constant number of elementary operations of $O(\log n)$ bits (e.g., accessing the $O(n)$ -th address, sampling one element from $O(n)$ elements). Therefore, if we assume that these operations can be done in constant time, the total computational complexity of our algorithms will be constant. This assumption is natural because most computers in the real-world can handle 64 bit integers at once and most of the network data contain less than $2^{64} \approx 10^{19}$ nodes.
- Even if the above assumption is not satisfied, our algorithm can be executed in $O(\log n)$ time in terms of the strict meaning of computational complexity. This indicates that our algorithm is still sub-linear and therefore it scales well. It should be noted that it is impossible to access even a single node in $o(\log n)$ time in the strict meaning of computational complexity because we cannot distinguish n nodes with $o(\log n)$ bits. Therefore, our algorithm has optimal complexity with respect to the number of nodes n .

Table 2. Time complexity of embedding algorithms. Δ denotes the maximum degree. It should be noted that in the dense graph, $O(m) = O(n^2)$ by definition.

	Sparse	Dense
Proposed	$O(\frac{1}{\varepsilon^{2L}} (\log \frac{1}{\varepsilon} + \log \frac{1}{\delta})^{L-1} \log \frac{1}{\delta})$	$O(\frac{1}{\varepsilon^{2L}} (\log \frac{1}{\varepsilon} + \log \frac{1}{\delta})^{L-1} \log \frac{1}{\delta})$
Exact	$O(\Delta^L)$	$O(mL) = O(n^2L)$

E. Graph Embedding

Our method can be extended to graph embedding, which embeds an entire graph instead of a node of a graph. It can be calculated by aggregating the embeddings of all nodes (Gilmer et al., 2017):

$$z_G = \text{READOUT}(\{z_i \mid i \in V\}).$$

We adopt the mean of the feature vectors of the nodes as the readout function (*i.e.*, $z_G = \frac{1}{n} \sum_{i \in V} z_i$). However, we cannot calculate the embeddings of all nodes in constant time even if each calculation is done in constant time because it takes a total of $\Omega(n)$ time. We adopt the sampling strategy here as well. We sample some nodes in a uniformly random manner, compute their feature vectors in constant time using Algorithm 2, and calculate their empirical mean. The errors of sampling and Algorithm 2 are bounded by Lemma 12 and Theorem 1, respectively. Therefore, we sample a sufficiently large (but independent of the graph size) number of nodes and call Algorithm 2 with sufficiently small ε and δ . Then, the estimate is arbitrarily close to the exact embedding of G with an arbitrary probability.

F. Time Complexity

We summarize the time complexity of approximation and exact algorithms in Table 2. Let $\mathcal{B}_L = \{v\}$ and $\mathcal{B}_l = \bigcup_{u \in \mathcal{B}_{l+1}} \mathcal{N}(u)$ ($l = 0, \dots, L - 1$). In other words, \mathcal{B}_{L-k} is the k -hop neighbors of node v . All features of \mathcal{B}_0 are required to calculate the exact embedding of node v . If the graph is sparse, the size of \mathcal{B}_{L-k} grows exponentially with respect to k because $\text{deg}(u)$ nodes are added to \mathcal{B}_{L-k+1} for each node $u \in \mathcal{B}_{L-k}$. Namely, it is bounded by Δ^k . If the graph is dense, $\mathcal{B}_{L-k} \approx \mathcal{V}$ ($1 \leq k \leq L$) Therefore, complexity is linear with respect to the number of layers L and edges m . In contrast, the approximation algorithm runs in constant time irrespective of the density of the input graph.